

Nonequilibrium persistent currents in mesoscopic disordered systems

Ph.D. thesis at SISSA

student: Oleg Chalaev

supervisor: Vladimir Kravtsov

examination date: 24.10.2003; last renewal 30.03.2009

(See the original version at <http://www.sissa.it/cm/thesis/2003/chalaev.ps.gz>)

Contents

1	Introduction	2
2	Current-current correlator in equilibrium	3
2.1	General relations	3
2.2	The short-range diagram	3
2.3	The long-range diagram	5
2.4	Charge conservation	6
2.5	The final result	7
3	Persistent current in a quasi-one-dimensional mesoscopic ring.	9
3.1	Thermodynamic and kinetic parts of a physical quantity	9
3.2	Thermodynamic persistent current	10
3.2.1	Calculation of Hartree diagram	11
3.2.2	The renormalization of the potential in the Cooper channel	14
3.3	Kinetic part of persistent current	15
3.3.1	Singlet channel	16
3.3.2	Triplet channel	18
3.3.3	Singlet channel in case of a $\delta(\vec{r} - \vec{r}')$ -like interaction	20
3.4	Result and its discussion	21
3.5	Discussion	22
3.6	Conclusions	23
4	Appendix	24
4.1	Trace of a thermodynamic current operator	24
4.2	Density matrix in quasiequilibrium state	24
4.3	Dephasing in the ring	25
4.4	Average of a Green's function	25
4.5	Average of two Green's functions: cooperon and diffuson	27
4.6	Keldysh technique	28
4.7	Screening	29
4.8	Other formulas	32

A technical note: the .pdf version of this document (obtained with the help of pdflatex) is more suitable for viewing on-line (since there are alive http links); If you want all http links to be printed, translate it with latex and then dvips.
The thesis is complementary to my notes, which are available on my homepage [1].

1 Introduction

Quantum effects in a physical system are often effects of interference of electrons. They can be seen if electrons remain coherent in the system, so that the size of the system $L < L_\phi$ = coherence length. The coherence can be destroyed by inelastic processes (electron-electron and electron-phonon interactions), being immune to elastic processes (scattering on impurities). By elastic we mean a process conserving energy of an electron.

Consider a system of an intermediate size: $l \ll L \ll L_\phi$, where l is the mean free path of an electron between scattering on impurities. Passing through the system, an electron gets scattered by impurities many times – so called diffusive regime. Still electrons maintain coherence so that we are able to observe beautiful quantum effects [2].

Consider a mesoscopic ring pierced by magnetic flux. Without taking interaction into account it is clear that all physical quantities will depend periodically on magnetic field: in fact, energy levels of such a system are flux-dependent, and the state of the system will be repeated every time an energy level passes through the Fermi level, because under the Fermi level there are still many energy levels left.

Once energy levels become flux dependent, a persistent current [3, 4] arises according to

$$\vec{j}(\vec{r}) = -\frac{\delta \bar{E}}{\delta \vec{A}(\vec{r})}, \quad \bar{E} = \int_{-E_F}^{\infty} dE \nu_E f_T(E) E = \sum_n f_T(E_n) E_n.$$

This current does not need electric field to be preserved, it is nonzero also in an equilibrium state.

An interesting part of mesoscopic physics is represented by nonequilibrium systems. Studying them is complicated by the fact that one has to take interaction into account. In fact, without interaction there would be no relaxation; both time directions in the system would be equivalent. The interaction produces relaxation, which is a cause for effects absent in equilibrium. The study of such effects is the main scope of this thesis.

We study persistent currents in mesoscopic systems in the diffusion regime with periodic boundary conditions¹. Our main tool in calculations is the disorder averaging technique [5, 6]. We consider an ensemble of many systems (or samples) having the same macroscopic characteristics. Each sample contains impurities that form scattering potential $U(r)$ for electrons; impurities are placed differently in different samples. Using disorder averaging technique [5, 6], we study averages over the ensemble of samples. The potential $U(r)$ is supposed to be delta-correlated:

$$\langle U(\vec{r}) U(\vec{r}') \rangle \stackrel{\text{df}}{=} (2\pi\nu_0\tilde{\tau})^{-1} \delta(\vec{r} - \vec{r}'), \quad (1)$$

where $\tilde{\tau}$ is the parameter characterizing the strength of disorder, and ν_0 is the density of states at the Fermi level. Eq. (1) reflects the assumption that the potential of every single impurity is independent from the others.

The text is divided into three main parts: in section 2 we study current-current correlator in a 2D system with periodic boundary conditions in magnetic field. The system is assumed to be in equilibrium and the interaction is not taken into account. It is interesting to note, that the anisotropy due to the applied external vector potential is strongly suppressed, so that the result is almost insensitive to the direction of \vec{A} .

The section 3 is devoted to the persistent current in mesoscopic rings out of equilibrium. At first, the thermodynamic part of the current is studied in section 3.2. Then, its kinetic part is calculated in sec. 3.3. Most part of calculations that alone do not lead to physical conclusions has been put in appendix (section 4). In particular, this includes expressions for cooperon, diffuson and screened Coulomb interaction for the case of energy-dependent density of states.

An important part of this thesis is the program² that strongly facilitates work with diagrams of the disorder averaging technique using Keldysh formalism. Its main function is generation of diagrams, selecting them (according to the loops number and other criteria) and drawing the selected diagrams. During our calculations, this program (written in *Mathematica*®) permitted enormous time savings.

¹Considering periodic boundary conditions is most convenient from the theoretical point of view.

²The program is now mostly obsolete. Its new version is completely rewritten on *maxima* and strongly extended. You can find it (together with examples and instructions for usage) on my homepage [1]. Note also that the original (24.10.2003) version of this document is permanently available on the SISSA CM page.

2 Current-current correlator in equilibrium

added 09.03.2005: In this section we did not include thermal fluctuations into the correlator. See the discussion on p. ?? of [7]. In addition the magnetic field is in-plane, so that we can neglect orbital motion of electrons, which is going to change Hamiltonian's eigensystem, and, consequently, Green's functions. Still I made the calculation for the case of homogeneous vector potential. This approximation is clearly justified for the quasi-onedimensional ring, but it is unclear why it could be used here as well. This was my very first mesoscopic calculation. Now I am skeptical about it.

Consider two-dimensional disordered mesoscopic system with periodic boundary conditions. An applied magnetic field generates circular persistent current in the system [8]. In this section we calculate its second momentum $\langle j_\alpha(\vec{r}) j_\beta(\vec{r}') \rangle$ in a two dimensional system with dimensions $L_x \times L_y$. In equilibrium interaction usually gives small correction to the main contribution of a physical quantity³, unless without the interaction the result is zero. Thus we can hope that it is safe to ignore interaction effects here.

The main contribution to the current correlator occurs from the first-loop diagrams in the disorder averaging technique.

2.1 General relations

From (A40) and (A41) we obtain formula for the current in case of no interaction between electrons:

$$\vec{j}(\vec{r}) = \int_{-\infty}^{\infty} \frac{dE}{2\pi} f_T(E) \vec{j}(\vec{r}, E), \quad f_T(E) = \frac{1}{1 + e^{E/T}}, \quad (2)$$

$$\vec{j}(\vec{r}, E) = \frac{e}{2m} \lim_{\vec{r}' \rightarrow \vec{r}} (\vec{\nabla}_{\vec{r}} - \vec{\nabla}_{\vec{r}'} - 2ie\vec{A}) [G_R(\vec{r}, \vec{r}'; E) - G_A(\vec{r}, \vec{r}'; E)], \quad (3)$$

From (A18) it follows that without interaction $[G_R(\vec{r}, \vec{r}'; E) - G_A(\vec{r}, \vec{r}'; E)] = 0$ for $E < -E_F$ (given that $E = 0$ corresponds to the Fermi level), so that the integral in (2) converges.

From (2), follows the expression for the second current moment:

$$\begin{aligned} \langle j_\alpha(\vec{r}) j_\beta(\vec{r}') \rangle &= \frac{e^2}{16\pi^2 m^2} \int_{-\infty}^{\infty} dE_1 dE_2 f_T(E_1) f_T(E_2) \lim_{\substack{\vec{r}_1, \vec{r}_3 \rightarrow \vec{r} \\ \vec{r}_2, \vec{r}_4 \rightarrow \vec{r}'}} \left(\frac{\partial}{\partial r_{1\alpha}} - \frac{\partial}{\partial r_{3\alpha}} - 2ieA_\alpha \right) \left(\frac{\partial}{\partial r_{2\beta}} - \frac{\partial}{\partial r_{4\beta}} - 2ieA_\beta \right) \times \\ &\quad \times [\langle G_R(\vec{r}_1, \vec{r}_3; E_1) G_A(\vec{r}_2, \vec{r}_4; E_2) \rangle + \langle G_A(\vec{r}_1, \vec{r}_3; E_1) G_R(\vec{r}_2, \vec{r}_4; E_2) \rangle]. \end{aligned} \quad (4)$$

The second term in square brackets in (4) can be obtained from the first one (and vice versa) by substituting: $\vec{r}_1 \leftrightarrow \vec{r}_2$, $\vec{r}_3 \leftrightarrow \vec{r}_4$ and $E_1 \leftrightarrow E_2$. This means that it gives the same contribution as the first one.

Within the first-loop approximation $\langle j_\alpha(\vec{r}) j_\beta(\vec{r}') \rangle$ is represented by four diagrams: two diagrams with cooperons (drawn in Fig. 1), and the other two with diffusons:

$$\begin{aligned} \langle j_\alpha(\vec{r}) j_\beta(\vec{r}') \rangle &= \frac{e^2}{8\pi^2 m^2} \int_{-\infty}^{\infty} dE_1 dE_2 f_T(E_1) f_T(E_2) \lim_{\substack{\vec{r}_1, \vec{r}_3 \rightarrow \vec{r} \\ \vec{r}_2, \vec{r}_4 \rightarrow \vec{r}'}} \left(\frac{\partial}{\partial r_{1\alpha}} - \frac{\partial}{\partial r_{3\alpha}} \right) \\ &\quad \left[\left(\frac{\partial}{\partial r_{2\beta}} - \frac{\partial}{\partial r_{4\beta}} \right) \langle G_R(\vec{r}_1, \vec{r}_3; E_1) G_A(\vec{r}_2, \vec{r}_4; E_2) \rangle_C + \left(\frac{\partial}{\partial r_{4\beta}} - \frac{\partial}{\partial r_{2\beta}} \right) \langle G_R(\vec{r}_1, \vec{r}_3; E_1) G_A(\vec{r}_4, \vec{r}_2; E_2) \rangle_D \right], \end{aligned}$$

where $\langle \dots \rangle_C$ and $\langle \dots \rangle_D$ denote contributions from cooperon and diffuson diagrams respectively.

In case of $\vec{A} = 0$ diffuson diagrams cancel cooperon ones, due to the reason that

$$\langle G_R(\vec{r}_1, \vec{r}_3; E_1) G_A(\vec{r}_2, \vec{r}_4; E_2) \rangle_C = \langle G_R(\vec{r}_1, \vec{r}_3; E_1) G_A(\vec{r}_4, \vec{r}_2; E_2) \rangle_D. \quad (5)$$

It is evident that the second diagram (i.e. b and d in Fig. 1) should give significant contribution to long-range correlations, while the first (a and c) does not.

In the following two sections we calculate diagrams in Fig. 1.

2.2 The short-range diagram

The short range diagram is drawn in Fig. 1a) and c):

$$\begin{aligned} \langle j_\alpha(\vec{r}) j_\beta(\vec{r}') \rangle_1 &= \frac{e^2}{8\pi^2 m^2} \int_{-\infty}^{\infty} dE d\omega f_T(E) f_T(E - \omega) \int d^d x_1 d^d x_2 C(\vec{x}_1, \vec{x}_2; \omega) \times \\ &\quad \left[\frac{\partial G_R(\vec{r}, \vec{x}_1)}{\partial r_\alpha} G_R(\vec{x}_2, \vec{r}) - G_R(\vec{r}, \vec{x}_1) \frac{\partial G_R(\vec{x}_2, \vec{r})}{\partial r_\alpha} - 2ieA_\alpha G_R(\vec{r}, \vec{x}_1) G_R(\vec{x}_2, \vec{r}) \right] \times \\ &\quad \left[\frac{\partial G_A(\vec{r}', \vec{x}_3)}{\partial r'_\beta} G_A(\vec{x}_4, \vec{r}') - G_A(\vec{r}', \vec{x}_3) \frac{\partial G_A(\vec{x}_4, \vec{r}')}{\partial r'_\beta} - 2ieA_\beta G_A(\vec{r}', \vec{x}_3) G_A(\vec{x}_4, \vec{r}') \right], \end{aligned} \quad (6)$$

³Out of equilibrium this is not correct; Taking interaction into account can drastically change the value of a physical quantity. An example is the current studied in sec. 3.2.

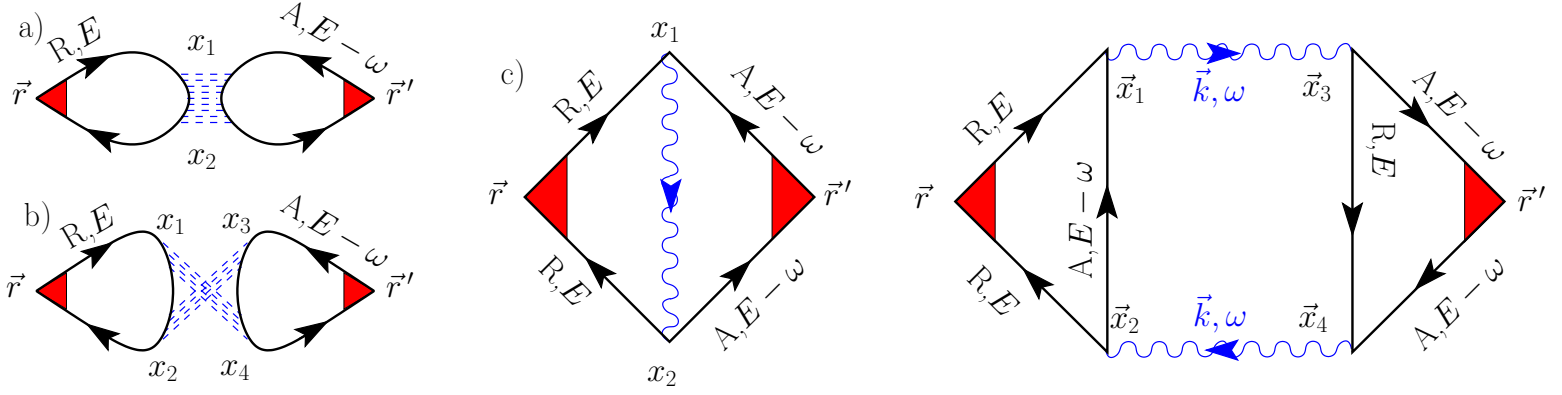


Figure 1: Two one-loop diagrams for $\langle \vec{j}(\vec{r}) \vec{j}(\vec{r}') \rangle$ drawn in two different ways: a) or c) is the short-range diagram, b) or d) is the long-range one. Straight lines denote Green functions; wavy lines denote cooperons.

where $C(\vec{x}_1, \vec{x}_2; \omega)$ denotes cooperon defined in (A29) in coordinate space. All G_R and G_A depend on energies E and $E - \omega$ respectively.

We have two spatial scales in our diagrams: l and L , $l \ll L$. We are interested in diffusion processes on scales larger than l ; Let us then approximate Hikami box (without cooperon) from the diagram in Fig. 1c (or two square brackets in (6)) with a combination of δ -functions:

$$K \delta(\vec{x}_2 - \vec{r}) \delta(\vec{x}_2 - \vec{r}') \delta(\vec{r} - \vec{x}_1) \delta_{\alpha\beta}. \quad (7)$$

There are four ways to write ansatz (7) in this form, but they are all equivalent. To find K , we integrate the square in Fig. 1c) by x_1 and x_2 :

$$K \delta_{\alpha\beta} \delta(\vec{r} - \vec{r}') = \int d^d x_1 d^d x_2 \left[\frac{\partial G_R(\vec{r}, \vec{x}_1)}{\partial r_\alpha} G_R(\vec{x}_2, \vec{r}) - G_R(\vec{r}, \vec{x}_1) \frac{\partial G_R(\vec{x}_2, \vec{r})}{\partial r_\alpha} - 2ieA_\alpha G_R(\vec{r}, \vec{x}_1) G_R(\vec{x}_2, \vec{r}) \right] \times \\ \times \left[\frac{\partial G_A(\vec{r}', \vec{x}_1)}{\partial r'_\beta} G_A(\vec{x}_2, \vec{r}') - G_A(\vec{r}', \vec{x}_1) \frac{\partial G_A(\vec{x}_2, \vec{r}')}{\partial r'_\beta} - 2ieA_\beta G_A(\vec{r}', \vec{x}_1) G_A(\vec{x}_2, \vec{r}') \right],$$

or, in momentum representation:

$$\int \frac{d^d p_1 d^d p_2}{(2\pi)^{2d}} (\vec{p}_1 + \vec{p}_2)_{\alpha\beta} \exp[i(\vec{r} - \vec{r}')(\vec{p}_1 - \vec{p}_2)] G_R(p_1) G_R(p_2) G_A(p_1) G_A(p_2) = \\ = 2\delta_l(\vec{r} - \vec{r}') \int \frac{d^d p}{(2\pi)^d} p_\alpha p_\beta G_R^2(p) G_A^2(p) = \frac{8}{d} \pi \nu \tau^3 p_F^2 \delta_{\alpha\beta} \delta_l(\vec{r} - \vec{r}'), \quad d = 2, \quad (8)$$

so that $K = 8\pi\nu\tau^3 p_F^2/d$. In (8) δ_l stands for the approximate delta-function $\delta_l(R) = \int_{-1/l}^{1/l} e^{ikR} dk$. Within the diffusion approximation, we can substitute δ_l with δ .

In section 4.1 we demonstrate that in (6) one can shift $f_T(E)$ by arbitrary constant; so, instead of Fermi distribution, we substitute $f_T(E) = -\frac{1}{2} \tanh \frac{E}{2T}$.

After applying ansatz (7), only energy integration remains in (6), and the shortest form it has in time representation:

$$\langle j_\alpha(\vec{r}) j_\beta(\vec{r}') \rangle_1 = K \delta_{\alpha\beta} \delta(\vec{r} - \vec{r}') \int_0^\infty dt g(t) C(\vec{r}\vec{r}'; t), \\ g_T(t) = \int_0^\infty dE \tanh \frac{E}{2T} \cdot \sin(Et) e^{-\epsilon t}, \quad \epsilon = +0, \quad g_0(t) = 1/t. \quad (9)$$

where $C(\vec{r}\vec{r}'; t)$ is the cooperon (A32) in coordinate representation. Later we omit index T in $g_T(t)$.

Using (A75), let us rewrite the result (9) in terms of Poisson harmonics:

$$C(\vec{r}\vec{r}'; t) = \frac{1}{2\pi\nu\tau^2 L_x L_y} \sum_{\vec{p}_k} \exp[-(\vec{p}_k - 2e\vec{A})^2 Dt] = \sum_{\vec{m}} \cos \left[2\pi \vec{m} \frac{\vec{\phi}}{\phi_0} \right] \frac{1}{8\pi^2 \nu Dt \tau^2} \exp \left[-\frac{y^2}{4Dt} \right],$$

where we used notations:

$$\vec{y} = (L_x m_x, L_y m_y)^T, \quad \vec{\phi} = (L_x A_x, L_y A_y)^T. \quad (10)$$

Finally we arrive to an expression

$$\langle j_\alpha(\vec{r}) j_\beta(\vec{r}') \rangle_1 = \sum_{\vec{m}} \cos \left[2\pi \vec{m} \frac{\vec{\phi}}{\phi_0} \right] \delta(\vec{r} - \vec{r}') \frac{e^2}{(2\pi)^3} \delta_{\alpha\beta} \int_0^\infty \frac{dt}{t} g^2(t) \exp \left[-\frac{y^2}{4Dt} \right]. \quad (11)$$

Note that the result (11) is invariant with respect to rotation of $\vec{\phi}/\phi_0$ by $\pi/2$. The contribution from the long range diagram (see the next section) does not possess such invariance.

2.3 The long-range diagram

The long-range diagram is drawn in Fig. 1b) and d). Its contribution to the current correlator is equal to

$$\begin{aligned} \langle j_\alpha(\vec{r})j_\beta(\vec{r}') \rangle_2 &= \frac{e^2}{8\pi^2 m^2} \int_{-\infty}^{\infty} dE d\omega f_T(E) f_T(E - \omega) \times \\ &\int d^d x_{1\dots 4} C(\vec{x}_1 \vec{x}_2; E_1) C(\vec{x}_3 \vec{x}_4; E_1) G_A(\vec{x}_4, \vec{x}_1) G_R(\vec{x}_2, \vec{x}_3) \times \\ &\left[\frac{\partial G_R(\vec{r}, \vec{x}_1)}{\partial r_\alpha} G_R(\vec{x}_4, \vec{r}) - G_R(\vec{r}, \vec{x}_1) \frac{\partial G_R(\vec{x}_4, \vec{r})}{\partial r_\alpha} - 2ieA_\alpha G_R(\vec{r}, \vec{x}_1) G_R(\vec{x}_4, \vec{r}) \right] \times \\ &\left[\frac{\partial G_A(\vec{r}', \vec{x}_3)}{\partial r'_\beta} G_A(\vec{x}_2, \vec{r}') - G_A(\vec{r}', \vec{x}_3) \frac{\partial G_A(\vec{x}_2, \vec{r}')}{\partial r'_\beta} - 2ieA_\beta G_A(\vec{r}', \vec{x}_3) G_A(\vec{x}_2, \vec{r}') \right]. \end{aligned} \quad (12)$$

Like we did it before, in (12) we shift $f_T(E_{12})$ by $\frac{1}{2}$, so that instead of Fermi distribution, we assume $f_T(E) = -\frac{1}{2} \tanh \frac{E}{2T}$. All G_R and G_A have energy E and $E - \omega$ correspondingly. In (12) Green functions and cooperon self energies are in the coordinate-energy representation. It is more convenient to work in momentum-time representation.

In analogy with what has been done in case of the short-range diagram, let us write approximate expressions for the triangulars with a combination of δ - functions:

$$\begin{aligned} G_A(\vec{x}_4, \vec{x}_1) &\left[\frac{\partial G_R(\vec{r}, \vec{x}_1)}{\partial r_\alpha} G_R(\vec{x}_4, \vec{r}) - G_R(\vec{r}, \vec{x}_1) \frac{\partial G_R(\vec{x}_4, \vec{r})}{\partial r_\alpha} - \right. \\ &\left. - 2ieA_\alpha G_R(\vec{r}, \vec{x}_1) G_R(\vec{x}_4, \vec{r}) \right] e^{2i\vec{A}(\vec{x}_4 - \vec{x}_1)} = \\ &Z\delta(\vec{r} - \vec{x}_1)\delta(\vec{x}_4 - \vec{r}) + J_\alpha \frac{\partial \delta(\vec{r} - \vec{x}_1)}{\partial r_\alpha} \delta(\vec{x}_4 - \vec{r}) - S_\alpha \delta(\vec{r} - \vec{x}_1) \frac{\partial \delta(\vec{x}_4 - \vec{r})}{\partial r_\alpha}. \end{aligned} \quad (13)$$

One can see that $Z = 0$.

For the left triangular in Fig. 1d we have:

$$\begin{aligned} J_\alpha &= - \int d^2 r_1 d^2 r_2 G_A(\vec{r}_1 + \vec{r}_2) r_{1\alpha} \left[\frac{\partial G_R(\vec{r}_1)}{\partial r_{1\alpha}} G_R(\vec{r}_2) + G_R(\vec{r}_1) \frac{\partial G_R(\vec{r}_2)}{\partial r_{2\alpha}} \right] = \\ S_\alpha &= - \int d^2 r_1 d^2 r_2 G_A(\vec{r}_1 + \vec{r}_2) r_{2\alpha} \left[\frac{\partial G_R(\vec{r}_1)}{\partial r_{1\alpha}} G_R(\vec{r}_2) + G_R(\vec{r}_1) \frac{\partial G_R(\vec{r}_2)}{\partial r_{2\alpha}} \right]. \end{aligned} \quad (14)$$

The expression for the right triangular in Fig. 1b can be obtained from (14) by substituting $\alpha \rightarrow \beta$, then G_R by G_A and vice versa. It is easier to calculate (14) in momentum representation. One can see that $J_\alpha = S_\alpha$ and they do not depend on α , because

$$\begin{aligned} \int d^d r_1 d^d r_2 G_A(r_1 + r_2) \frac{\partial G_R(r_2)}{\partial r_{2\alpha}} G_R(r_1) r_{2\alpha} \int d^d r_1 d^d r_2 G_A(r_1 + r_2) \frac{\partial G_R(r_2)}{\partial r_{2\alpha}} G_R(r_1) r_{1\alpha} = \\ - \int \frac{d^d p}{(2\pi)^d} G_A(\vec{p}) p_\alpha G_R(\vec{p}) \frac{\partial G_R(\vec{p})}{\partial p_\alpha} = \frac{2\pi\nu\tau^3 p_F^2}{md}, \quad d = 2, \end{aligned}$$

so that $J_\alpha = S_\alpha = -4\pi\nu\tau^2 p_F l / d \equiv J$.

Like in sec. 2.2, let us switch to time representation:

$$\begin{aligned} \langle j_\alpha(\vec{r})j_\beta(\vec{r}') \rangle_2 &= J^2 \frac{e^2}{8\pi^2 m^2} \int_0^\infty dt_1 dt_3 g^2(t_1 + t_3) \lim_{\substack{\vec{x}_1, \vec{x}_4 \rightarrow \vec{r} \\ \vec{x}_2, \vec{x}_3 \rightarrow \vec{r}'}} \left(\frac{\partial}{\partial x_{1\alpha}} - \frac{\partial}{\partial x_{4\alpha}} \right) \times \\ &\left(\frac{\partial}{\partial x_{3\beta}} - \frac{\partial}{\partial x_{2\beta}} \right) \exp \left[-2ie\vec{A}(\vec{x}_1 - \vec{x}_2 + \vec{x}_3 - \vec{x}_4) \right] C(\vec{x}_1 \vec{x}_2; t_1) C(\vec{x}_3 \vec{x}_4; t_3), \end{aligned} \quad (15)$$

where $C(\vec{x}_1 \vec{x}_2; t_1)$ and $C(\vec{x}_3 \vec{x}_4; t_3)$ are cooperons (A32) in coordinate-time representation.

Then let us rewrite (15) in momentum-time representation:

$$\begin{aligned} \exp \left[-2ie\vec{A}(\vec{x}_1 - \vec{x}_2 + \vec{x}_3 - \vec{x}_4) \right] C(\vec{x}_1 \vec{x}_2; t_1) C(\vec{x}_3 \vec{x}_4; t_3) = \\ \sum_{\vec{q}_{n1}, \vec{q}_{n2}} \exp \left[i\vec{q}_{n1}(\vec{x}_1 - \vec{x}_2) - 2ie\vec{A}(\vec{x}_1 - \vec{x}_2) \right] \exp \left[i\vec{q}_{n2}(\vec{x}_3 - \vec{x}_4) - 2ie\vec{A}(\vec{x}_3 - \vec{x}_4) \right] \times \\ \left(\frac{1}{2\pi\nu\tau^2} \right)^2 \frac{1}{(L_x L_y)^2} \exp \left[-(\vec{q}_{n1} - 2e\vec{A})^2 D t_1 \right] \exp \left[-(\vec{q}_{n2} - 2e\vec{A})^2 D t_3 \right]. \end{aligned} \quad (16)$$

Inserting (16) into (15) and making substitutions $\vec{R}_1 = \vec{x}_1 - \vec{x}_2$, $\vec{R}_2 = \vec{x}_4 - \vec{x}_3$, $\vec{R} = \vec{r} - \vec{r}'$ and then $\vec{q}_n = \vec{q}_{n1} - \vec{q}_{n2}$, $\vec{q}_{n1} \rightarrow \vec{p}_k$, one obtains the spatial structure of (15) (that is, its part after $g^2(t_1 + t_3)$):

$$-\frac{1}{(L_x L_y)^2} \frac{1}{(2\pi\nu\tau^2)^2} \sum_{\vec{q}_n} \exp[i\vec{R}\vec{q}_n] \times \sum_{\vec{p}_k} (2\vec{p}_k - 4e\vec{A} - \vec{q}_n)_{\alpha\beta} \times \exp\left[-(\vec{p}_k - 2e\vec{A})^2 Dt_1 - (\vec{p}_k - 2e\vec{A} - \vec{q}_n)^2 Dt_3\right]. \quad (17)$$

where two indices denote diadic: $p_{\alpha\beta} \equiv p_\alpha p_\beta$.

It is evident that $\langle j_\alpha(\vec{r}) j_\alpha(\vec{r}') \rangle = \langle j_\alpha(\vec{r}') j_\alpha(\vec{r}) \rangle$, like that the substitution $\vec{r} \leftrightarrow \vec{r}'$ is equivalent to $\vec{A} \rightarrow -\vec{A}$. From these two statements it follows that the correlator should not depend on the sign of \vec{A} . One can prove it using the symmetry⁴ in integration by t_1 and t_3 and then (after the change of variables from t_1 and t_3 to τ_1 and τ_2 , see (18)) the fact that the integration by τ_2 is performed in symmetrical limits.

From (A75) we deduce that $\sum_{\vec{p}_k}$ in (17) is equal to

$$\frac{L_x L_y}{(2\pi)^2} \sum_{\vec{m} \in \mathbb{Z}^2} \exp\left[2\pi i \vec{m} \cdot \left(\frac{\vec{\phi}}{-\phi_0}\right)\right] \int \exp(i\vec{y}\vec{p}) f_{\alpha\beta}(\vec{p}) d^2 p,$$

where the integral is taken in (A76); \vec{y} and $\vec{\phi}$ are defined in (10). According to (A77), it is convenient to introduce new variables⁵:

$$Dt_1 + Dt_3 = \tau_1, Dt_1 - Dt_3 = \tau_2. \quad (18)$$

Then

$$\begin{aligned} \langle j_\alpha(\vec{r}) j_\beta(\vec{r}') \rangle_2 = & -\frac{1}{L_x L_y} \frac{e^2 (p_F l)^2}{8m^2} \sum_{\vec{q}_n} e^{i\vec{q}_n(\vec{r}-\vec{r}')} \frac{1}{(2\pi)^3} \sum_{\vec{m}} \exp\left[2\pi i \vec{m} \cdot \frac{\vec{\phi}}{-\phi_0}\right] \times \\ & \int_0^\infty \frac{d\tau_1}{D} \frac{g^2(\tau_1)}{\tau_1^2} \exp\left[-\frac{(\tau_1 \vec{q} - i\vec{y})^2}{4\tau_1}\right] \exp\left[-\frac{y^2}{2\tau_1}\right] \times \\ & \int_{-\tau_1}^{\tau_1} \frac{d\tau_2}{D} \left(\delta_{\alpha\beta} + \frac{1}{2\tau_1} [\tau_2 \vec{q} - i\vec{y}]_{\alpha\beta}\right) \exp\left[\frac{\tau_2^2 q^2 - 2i\tau_2 \vec{y}\vec{q}}{4\tau_1}\right]. \end{aligned} \quad (19)$$

Due to the fact that $\sin\left[\frac{\vec{q}\vec{y}}{2}\right] = 0$, (19) is invariant with respect to the substitution $\vec{q} \rightarrow -\vec{q}$; thus $e^{i\vec{q}_n(\vec{r}-\vec{r}')}$ in (19) can be changed to $\cos[\vec{q}_n(\vec{r}-\vec{r}')]$.

2.4 Charge conservation

As a consequence of charge conservation law $\text{div } \vec{j}(\vec{r}) = 0$, second moment of the current must obey the restriction:

$$\sum_{\beta=1}^2 q_\beta \langle j_\alpha(\vec{q}) j_\beta(\vec{q}) \rangle = 0, \quad \alpha = 1, 2. \quad (20)$$

Let us see how (20) holds for (11) and (19). The application of (20) to the last integral $\int_{-\tau_1}^{\tau_1} \frac{d\tau_2}{D}$ in (19) leads to an equation:

$$0 = \int_{-\tau_1}^{\tau_1} \frac{d\tau_2}{D} \left(\vec{q} + \frac{1}{2\tau_1} \vec{Q} \vec{q} \vec{Q}\right) \exp\left[\frac{\tau_2^2 q^2 - 2i\tau_2 \vec{y}\vec{q}}{4\tau_1}\right] = \frac{2\tau_1 \vec{q}}{D} \exp\left[\frac{\tau_1 q^2}{4}\right] \cos\left[\frac{\vec{q}\vec{y}}{2}\right], \quad (21)$$

where $\vec{Q} = \tau_2 \vec{q} - i\vec{y}$. In (21) we performed integration by parts, using the fact that

$$\frac{\partial}{\partial \tau_2} \exp\left[\frac{\tau_2^2 q^2 - 2i\tau_2 \vec{y}\vec{q}}{4\tau_1}\right] = \frac{1}{2\tau_1} \vec{q} \vec{Q} \exp\left[\frac{\tau_2^2 q^2 - 2i\tau_2 \vec{y}\vec{q}}{4\tau_1}\right] \quad (22)$$

From (21) we conclude that the expression (19) for the long-range diagram in Fig. 1b) can be divided in two parts. The first part obeys charge conservation law; this means its Fourier \vec{q} -harmonic can be written in the form $f(\vec{q}) \left[\delta_{\alpha\beta} - \frac{q_\alpha q_\beta}{q^2}\right]$, where $f(\vec{q})$ is an arbitrary scalar function.

The second part can not be proportional to $\delta_{\alpha\beta}$ because then the charge conservation law (20) gets inevitably violated. The only possibility to save the conservation law is to assume that it is proportional to $\frac{q_\alpha q_\beta}{q^2}$; then, together with the contribution of

⁴To see this one should make in (17) a substitution $\vec{p}_k \rightarrow \vec{p}_k - \vec{q}_n$.

⁵The multiplier = 1/4 appears due to this substitution.

the short-range diagram (11), it can form an expression $f^S(\vec{q})\delta_{\alpha\beta} - f^L(\vec{q})\frac{q_\alpha q_\beta}{q^2}$, which will ensure charge conservation law (20), given $f^S = f^L$. From (11), (19) and (21) one can see that this is really the case, so that we can rewrite (19) in the form:

$$\begin{aligned} \langle j_\alpha(\vec{r})j_\beta(\vec{r}') \rangle_2 = & -\frac{1}{L_x L_y} \frac{e^2(p_F l)^2}{4m^2 D^2} \frac{1}{(2\pi)^3} \sum_{\vec{q}_n} \cos[\vec{q}_n(\vec{r} - \vec{r}')] \\ & \int_0^\infty d\tau_1 \frac{g^2(\tau_1)}{\tau_1} \exp\left[-\frac{(\tau_1 \vec{q} - i\vec{y})^2}{4\tau_1}\right] \exp\left[-\frac{y^2}{2\tau_1}\right] \times \\ & \left\{ \left(\delta_{\alpha\beta} - \frac{q_\alpha q_\beta}{q^2} \right) \int_{-\tau_1}^{\tau_1} \frac{d\tau_2}{2\tau_1} \exp\left[\frac{\tau_2^2 q^2 - 2i\tau_2 \vec{y} \vec{q}}{4\tau_1}\right] + \frac{q_\alpha q_\beta}{q^2} \exp\left[\frac{\tau_1 q^2}{4}\right] \cos\left[\frac{\vec{y} \vec{q}}{2}\right] \right\}. \end{aligned} \quad (23)$$

2.5 The final result

From (11) and (23) we see that the \vec{q}_n harmonic of our correlator has the form

$$\begin{aligned} \langle j_\alpha(\vec{r})j_\beta(\vec{r}') \rangle = & \sum_{\vec{m} \neq 0} \left[\cos\left(2\pi \vec{m} \frac{\vec{\phi}}{\phi_0}\right) - 1 \right] \frac{1}{L_x L_y} \sum_{\vec{q}_n \neq 0} \cos[\vec{q}_n(\vec{r} - \vec{r}')] \left(\delta_{\alpha\beta} - \frac{q_\alpha q_\beta}{q^2} \right) \times \\ & \frac{e^2}{(2\pi)^3} \int_0^\infty \frac{dt}{t} g^2(t) \exp\left[-\frac{y^2}{4Dt}\right] \left\{ 1 - \frac{1}{2t} \int_{-t}^t dt' \exp\left[\frac{D(t'^2 - t^2)q^2 - 2i(t' - t)\vec{y} \vec{q}}{4t}\right] \right\}, \\ g(t) \equiv g_T(t) = & \int_0^\infty dE \tanh \frac{E}{2T} \cdot \sin(Et) e^{-\epsilon t}, \quad \epsilon = +0, \quad g_0(t) = 1/t, \\ \vec{y} = & (L_x m_x, L_y m_y)^T, \quad \vec{\phi} = (L_x A_x, L_y A_y)^T. \end{aligned} \quad (24)$$

For $T = 0$ the second string in (24) can be rewritten as

$$\begin{aligned} & \frac{e^2}{(2\pi)^3} \int_0^\infty \frac{dt}{t^3} g^2(t) \exp\left[-\frac{\tau_L}{t}\right] \times \\ & \left\{ 1 - \frac{1}{2t} \int_{-t}^t dt' \exp\left[\frac{t'^2 - t^2}{t\tau_q}\right] \exp\left[-2i\left(\frac{t'}{t} - 1\right) \frac{\vec{y} \vec{q} \tau_{Lq}}{yq \tau_q}\right] \right\}, \end{aligned} \quad (25)$$

where $\tau_L = m^2 L^2 / 4D$, $\tau_q = 4/Dq^2$, and $\tau_{Lq} = \sqrt{\tau_L \tau_q} = mL/Dq$. The integral in curved brackets has asymptotic

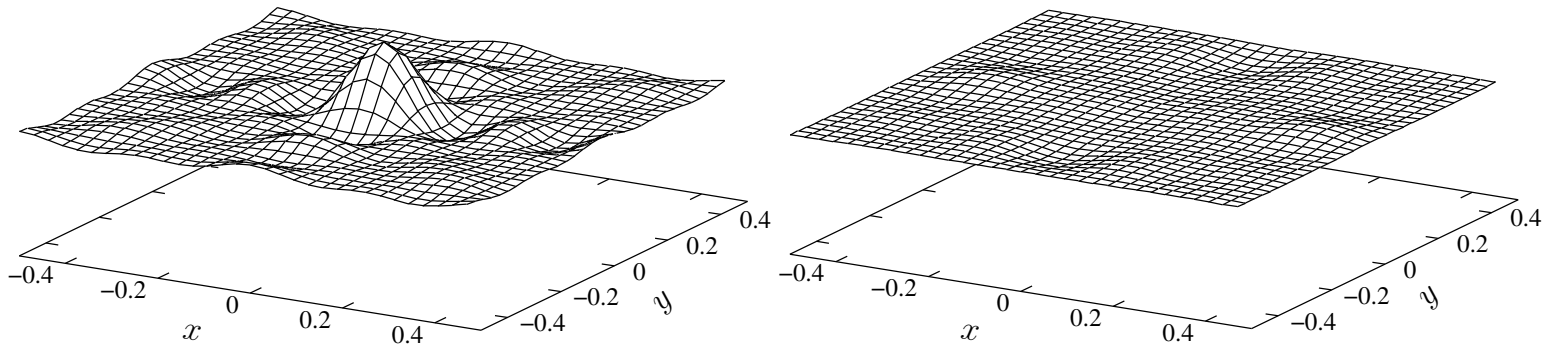
$$\frac{1}{2} \int_{-1}^1 dx \exp\left[\frac{t}{\tau_q}(x^2 - 1) - 2i(x - 1) \frac{\vec{y} \vec{q} \tau_{Lq}}{yq \tau_q}\right] \sim \frac{t/\tau_q}{\left(\frac{t}{\tau_q}\right)^2 + \left(\frac{\vec{y} \vec{q} \tau_{Lq}}{yq \tau_q}\right)^2}, \quad \frac{t}{\tau_q} \gg 1.$$

The integrand in (25) differs from zero for $t \gtrsim \tau_L$. One can check that always $\tau_q < \tau_{Lq} < \tau_L$. The higher Poisson (\vec{m}) and Fourier (\vec{q}) harmonics are considered, the stronger these inequalities are, and more isotropic their contribution to the correlator becomes. This is just what we see in Fig. 2: for small distances $|\vec{r} - \vec{r}'| \ll L$, where the higher Fourier harmonics are important, the correlator is isotropic; in the vicinity of the boundaries $|\vec{r} - \vec{r}'| \lesssim L$ some anisotropy arises.

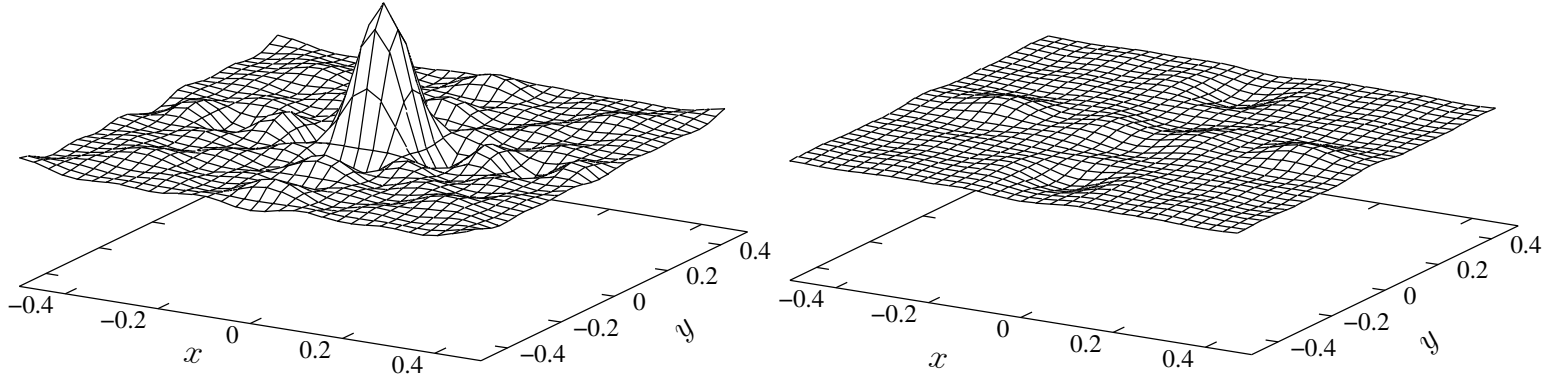
To conclude, the current correlator depends on the direction of the vector potential, but the dependence is weak, and there is no analytical parameter that controls it. Taking interaction into account can make this dependence more pronounced.

The current correlator was calculated numerically in [8]; no dependence on the direction of \vec{A} was observed when the interaction was neglected. This dependence became evident once the interaction was switched on. The authors concluded that there exist a transition between the situations with equilibrium and without equilibrium.

On the contrary, we sustain that (numerically) weak dependence on the direction of \vec{A} exists also in the case without the interaction; thus there is no transition, but just a crossover between the system with and without interaction.



(a) 16 Fourier and Poisson harmonics summed.



(b) 25 Fourier and Poisson harmonics summed.

Figure 2: On the left: current-current correlator in coordinate space, $T = 0$. The vector potential is directed along the y axis: $\vec{\phi}/\phi_0 = (0, 1/3)$. On the right: the difference between correlators calculated for $\vec{\phi}/\phi_0 = (0, 1/3)$ and $\vec{\phi}/\phi_0 = (1/3, 0)$. The correlator seem to have the symmetry the quadratic lattice it has been calculated on; the direction of vector potential seems irrelevant. Both center peak and anisotropy become more profound with enlargement of the number of summed harmonics.

3 Persistent current in a quasi-onedimensional mesoscopic ring.

Consider a mesoscopic ring made of impure metal or semiconductor. If it is pierced by static magnetic flux, then persistent current flows along the ring [3, 4]. This current does not require any electric field and is a manifestation of quantum interference effects. The direction and amplitude of the current depends on spatial distribution of impurities and varies from sample to sample. Given the circumference L of a ring is much larger than the mean path between collisions, the average persistent current is exponentially small [9] in a system without interaction⁶. In equilibrium case it was studied in ref. [10].

The case when the equilibrium is broken by the external ac field has been studied in [11]. The external field acted as a *direct* force acting on an electron system connected to an equilibrium reservoir. This force kept the system out of the equilibrium, while the reservoir maintained stable the energy distribution. Here we consider another type of non-equilibrium steady state. In our case the energy distribution of the reservoir is non-equilibrium, and there is no external ac field acting directly on the electron system.

Out of equilibrium, any physical quantity has two contributions: thermodynamic and kinetic (see the definition below). The kinetic part vanishes in equilibrium. In the considered situation, when there is no external ac force acting on electrons, it also equals zero without taking interaction into account; this is because relaxation becomes its driving force.

During the calculations we consider diagrams in the first order of perturbation theory. In addition, we take into account the renormalization of interaction in the Cooper channel (see sec. 3.2.2) and RPA (see sec. 4.7). More careful approach is described elsewhere (see ref. [12]).

When we perform calculations in momentum space, we calculate three dimensional sums over momentum like $\frac{1}{V} \sum_{\vec{k}}$. In momentum representation, all three components of momentum in the ring are quantized. For simplicity we consider quasi-onedimensional ring, that is, a ring with a cross-section $S \ll L^2$, where L is the ring's circumference. Then the quantum $2\pi/L$ of a component of momentum k_x , directed along the ring is much smaller than that for other two components k_y and k_z . Because of this, in three dimensional sums $\frac{1}{V} \sum_{\vec{k}}$, we can sum only over the component of momentum k_x along the ring's circumference. In the sums over k_y and k_z , we can leave only the term with $k_y = 0$ and $k_z = 0$; the contribution of the others produces small correction of the order of S/L^2 .

3.1 Thermodynamic and kinetic parts of a physical quantity

The stability of a non-equilibrium steady state is achieved by putting considered system in a contact with a reservoir - another system large enough so that its characteristics can not be modified by the considered system. The reservoir adds a compensating term into the Neyman equation for the density matrix of the system:

$$\frac{d\hat{\rho}}{dt} = \left. \frac{\partial \hat{\rho}}{\partial t} \right|_{\text{int}} + \left. \frac{\partial \hat{\rho}}{\partial t} \right|_{\text{ext}} = \frac{i}{\hbar} [\hat{\rho}, \hat{H}] + \left. \frac{\partial \hat{\rho}}{\partial t} \right|_{\text{ext}} = 0, \quad (26)$$

where $\left. \frac{\partial \hat{\rho}}{\partial t} \right|_{\text{ext}}$ characterizes the power of the connection of the system to the reservoir, necessary to maintain nonequilibrium steady state with a given energy distribution.

The average value of an arbitrary physical quantity \hat{O} can be written in the form

$$O = \text{Sp} [\hat{\rho} \hat{O}] = \text{Sp} [\hat{\rho}' \hat{O}'] + \text{Sp} [\hat{\rho}'' \hat{O}''] = O' + O'', \quad (27)$$

where $\hat{\rho}'$, \hat{O}' and $\hat{\rho}''$, \hat{O}'' denote diagonal and off-diagonal parts of matrices $\hat{\rho}$, \hat{O} .

The diagonal part $\hat{\rho}'$ of the density matrix $\hat{\rho}$ has the maximal entropy possible for the given energy distribution f_E (see the proof in sec. 4.2). With $\hat{\rho}'$ one can formally calculate thermodynamic functions like grand thermodynamic potential Ω and use thermodynamic formulas for the calculation of physical quantities. For this reason we call the term $O' = \text{Sp} [\hat{\rho}' \hat{O}']$ in (27) thermodynamic one. E.g., for thermodynamic part of the persistent current we have

$$\vec{j}' = \text{Sp} [\hat{\rho}' \hat{j}'] = -\frac{\partial \Omega}{\partial \vec{A}}, \quad (28)$$

Ω being the thermodynamic potential.

In equilibrium only diagonal matrix elements of a physical quantity enter into the expression for its average value, and thermodynamic part of a physical quantity is equal to its real value.

The separation of a physical quantity into its thermodynamic and kinetic parts can be formally done in Keldysh technique [13], just like in terms of density matrix (27). Let us demonstrate it for the case of the current density. The current density \vec{j} is expressed in terms of the Keldysh component G_K of 2×2 matrix Green function [14] $G = \begin{pmatrix} G_R & G_K \\ 0 & G_A \end{pmatrix}$:

$$\vec{j} = \text{Sp} \hat{j} G_K, \quad (29)$$

⁶This statement is true for the grand-canonical ensemble.

where G_K can be divided in two parts:

$$G_K = G'_K + G''_K, \quad G'_K(E) = h_E [G_R(E) - G_A(E)], \quad (30)$$

where $h_E = 1 - 2f_E$.

In equilibrium or without interaction $G_K(E) = h_E [G_R(E) - G_A(E)]$ (see (A41)), so that $G''_K = 0$ and $G_K = G'_K$. Out of equilibrium, the interaction generates off-diagonal elements in density matrix together with corrections to diagonal ones.

Applying the current operator to (30), we see that the current can be divided into the sum of thermodynamic and kinetic contributions:

$$\vec{j} = \text{Sp} \hat{j} G_K = j' + j''. \quad (31)$$

Let us analyze the expressions for j' and j'' in the first order of the perturbation theory in interaction. The correction to G due to the interaction is given by two terms (corresponding to Hartree and Fock diagrams⁷):

$$\delta G = -\frac{i}{2} \sum_{kk'} U_{kk'}(0) G(p) \tilde{\gamma}^k G(p) \text{Sp} \left[\int d^d q G(q) \gamma^{k'} \right] + \frac{i}{2} \sum_{kk'} \int d^d q U_{kk'}(q) G(p) \tilde{\gamma}^k G(p-q) \gamma^{k'} G(p), \quad (32)$$

$$\gamma_{ik}^1 = \sigma_1^{ik}, \quad \gamma_{ik}^2 = \delta_{ik}, \quad \tilde{\gamma}_{ik}^1 = \delta_{ik}, \quad \tilde{\gamma}_{ik}^2 = \sigma_1^{ik}, \quad (33)$$

where σ_1 is the Pauli matrix (??).

From (30) and (31) we obtain the expressions for j' and j'' :

$$\begin{aligned} j'' &= \frac{1}{2} \{ (\mathbf{AAR} - \mathbf{RAR}) [(h_E - h_{E-\omega}) U_\omega^K - (1 - h_E h_{E-\omega}) (U_\omega^R - U_\omega^A)] \}, \\ j' &= \frac{1}{2} A \{ \mathbf{RR} (U_\omega^R - 2U_0^R) (1 - h_E h_{E-\omega}) + \mathbf{RAA} (U_\omega^A - 2U_0^A) (1 - h_E h_{E-\omega}) \\ &\quad + (\mathbf{RRR} - \mathbf{AAA}) h_E U_\omega^K - (1 - h_E h_{E-\omega}) [\mathbf{RRR} (U_\omega^R - 2U_0^R) + \mathbf{AAA} (U_\omega^A - 2U_0^A)] \}, \end{aligned} \quad (34)$$

In (34), R and A denote G_R and G_A ; bold stands for the position of the current vertex, so that, for example, $\mathbf{AAR} \equiv G_0^A(E - \omega) G_0^A(E) \hat{j} G_0^R(E)$; the integration over E and ω is assumed. The factors 2 in the expression for j'' in (34) occurred due to the spin trace in Hartree terms. Looking on expressions (34), one notices that in thermodynamic terms, the vertex is placed between Green functions of the same type (both retarded or both advanced), while in kinetic terms it is placed between G_A and G_R . This is connected with the fact that, according to (28), diagrams for j' can be obtained by differentiating diagrams for the thermodynamic potential Ω . The diagrams for Ω do not contain vertices [5]. Taking derivative is equivalent to cutting the Green function line (G_R or G_A) in two, inserting the vertex in between. It is clear that such procedure can not produce diagrams with a vertex between different two different Green functions.

3.2 Thermodynamic persistent current

The thermodynamic part of the persistent current was calculated in [10] in equilibrium. In this section we recalculate it for more general non-equilibrium case.

The thermodynamic part j' of the current is given by (31). It follows from (A40) and (31) that

$$\vec{j}(\vec{r}) = \int dE f_T(E) \vec{j}(\vec{r}, E), \quad f_T(E) = \frac{1 - h_E}{2}, \quad (35)$$

$$\vec{j}(\vec{r}, E) = \frac{e\hbar}{2m} \lim_{\vec{r}' \rightarrow \vec{r}} (\vec{\nabla}_{\vec{r}} - \vec{\nabla}_{\vec{r}'} - 2ie\vec{A}) [G_R - G_A](\vec{r}, \vec{r}'; E), \quad (36)$$

where $f_T(E)$ is the energy distribution function. When Green functions depend only on the difference of their coordinates, (36) simplifies to

$$\begin{aligned} \vec{j}(\vec{r}, E) &= \vec{j}(E) = ie\hbar v \frac{1}{V} \sum_{\vec{p}_n} [G_R(\vec{p}_n, E) - G_A(\vec{p}_n, E)] = \\ &= -\hat{j}(\vec{p}) \frac{1}{V} \sum_{\vec{p}_n} [G_R(\vec{p}_n, E) - G_A(\vec{p}_n, E)], \quad \hat{j}(\vec{p}) \stackrel{\text{df}}{=} -i \frac{e\hbar}{m} \vec{p} \approx -ie\vec{v}. \end{aligned} \quad (37)$$

In (37) one must insert expressions for diagonal components $G_{R/A}$ of matrix Green function G obtained in Keldysh technique (see sec. 4.6).

⁷Note that Sp is taken also on spin degree of freedom in (32).

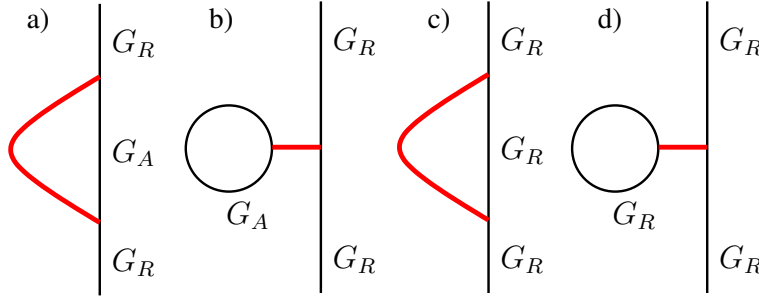


Figure 3: Diagrams for δG_R without cooperon and diffuson lines. Thin lines denote Green functions; thick lines stands for interaction.

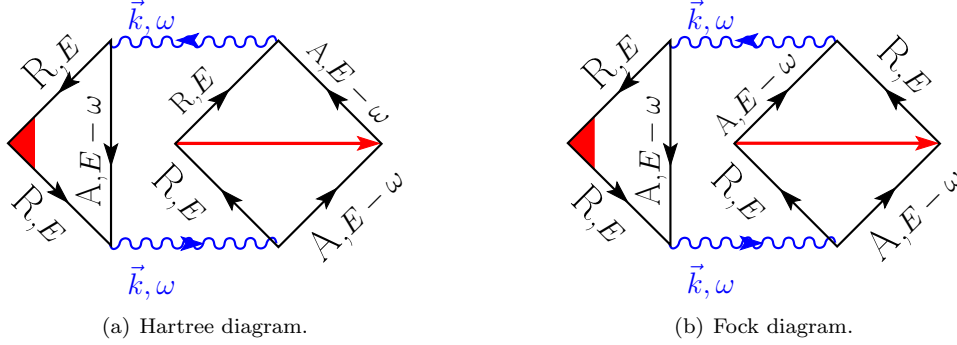


Figure 4: Diagrams for the current, obtained from fig. 3 by addition of cooperon lines (denoted by wavy lines); the coefficients are: $ih_{E-\omega}U_R(0)$ and $-ih_{E-\omega}U_R(\omega)/2$. One can note that (given the momentum transferred via the interaction line is large) these diagrams are equivalent. The triangulars are equal to $-4\pi\nu D\tau^3\vec{k}/l$.

From (32) we extract the expression for $\delta G_R - \delta G_A$:

$$\begin{aligned} \delta G_R - \delta G_A \equiv \delta (G_{11} - G_{22}) = \int \frac{d\omega}{2\pi} \int dydz \left\{ -iG_A^E(x, y)G_A^E(y, x)G_A^{E'}(z, z)h_{E'}U_{R/A}^0(y, z) + \right. \\ \left. iG_A^{E'}(z, z)G_R^E(x, y)G_R^E(y, x)h_{E'}U_{R/A}^0(y, z) - \frac{i}{2}G_A^E(x, y)G_A^E(z, x)G_R^{E-\omega}(y, z)h_{E-\omega}U_A^\omega(y, z) + \right. \\ \left. \frac{i}{2}G_A(x, y, e)G_A^{E-\omega}(y, z)G_A(z, x, e)[h_{E-\omega}U_A^\omega(y, z) - U_K^\omega(y, z)] - \text{c.c.} \right\} \end{aligned} \quad (38)$$

As a result, we obtain four initial diagrams drawn in Fig. 3. Two of them contain only G_R or only G_A so that one can not insert cooperon or diffuson lines in them. Due to this they can not depend on \vec{A} and thus cannot give any contribution to the current. Then we have 1 Hartree and 1 Fock diagram left, see fig. 3 b) and a).

According to the disorder averaging technique, the most important diagrams are those with the minimal number of loops and maximal number of centers (that is, bunches of Green's functions). In the first loop approximation, the main contribution is given by diagrams of Ambegaokar & Eckern [10] (Hartree and Fock ones) depicted in Fig. 4.

Looking on the diagrams in Fig. 4, we see that every pair of points in the squares can be connected by a path consisting only of Green function lines. In coordinate space, Green functions (A10) decay exponentially: $G_{R/A}(\vec{r} - \vec{r}') \propto \exp \frac{|\vec{r} - \vec{r}'|}{l}$, where mean free path l is the smallest spatial scale of the disorder averaging technique. Thus the diagrams can be significant only when their interaction lines are short-range, or, in other words, when they carry large values of momentum $\gtrsim 1/l$. Given this, the only difference between diagrams in Fig. 4(a) and 4(b) consists in the factor -2 . As we pointed out before, 2 arises from the spin trace in the Hartree diagram. By application of strong magnetic field, directed along the ring's circumference, one can polarize spins of electrons. Then the spin trace would produce 1 instead of 2, so that Hartree diagram would cancel the Fock one.

3.2.1 Calculation of Hartree diagram

Let us calculate the Hartree diagram; the Fock one is two times smaller and has the opposite sign, so that the final answer will be just half of the Hartree diagram (as it is pointed out in the end of the previous subsection). The Hartree current density is equal to

(see fig. 4)

$$j_H = \int_{-\infty}^{\infty} \frac{dE d\omega}{(2\pi)^2} f_E \frac{1}{V} \sum_{\vec{k}'_n} (iev) 2i \Im h_{E-\omega} \frac{\Lambda}{\nu} (-4\pi\nu D \tau^3 \vec{k}'/l) \frac{(2\pi\nu\tau)^2}{(2\pi\nu\tau^2)^2} \frac{1}{(Dk_n'^2 - i\omega)^2} =$$

$$\int_{-\infty}^{\infty} \frac{dE d\omega}{(2\pi)^2} f_E \frac{1}{V} \sum_{\vec{k}'_n} 2ev h_{E-\omega} (4\pi\nu D \tau k'/l) \frac{\Lambda}{\nu} \Im i \frac{1}{D^2(k_n'^2 + L_\omega^{-2})^2}, \quad (39)$$

where $\sum_{\vec{k}'_n}$ denotes the sum over $k'_n = 2\pi n/L - 2eA$, $n \in \mathbb{Z}$, and

$$L_\omega = \frac{1 + i \operatorname{sign} \omega}{\sqrt{2}} \sqrt{\frac{D}{|\omega|}}, \quad (40)$$

where $f_E = (1 - h_E)/2$ is the energy distribution function. Since the ring is assumed to be quasi-one-dimensional, the summation is performed only in one momentum component. Now we introduce Poisson summation:

$$\frac{1}{V} \sum_{\vec{k}'_n} \frac{k'_n}{(k_n'^2 + L_\omega^{-2})^2} = -\frac{1}{S} \sum_{n \in \mathbb{Z}} \exp \left[2\pi i n \frac{\Phi}{\Phi_0} \right] \int \frac{dk}{2\pi} \frac{\exp[iknL]}{k^2 + L_\omega^{-2}} =$$

$$\frac{2}{S} \sum_{n>0} \sin \left[2\pi n \frac{\Phi}{\Phi_0} \right] \int \frac{dk}{2\pi} \frac{\sin[knL]}{(k^2 + L_\omega^{-2})^2},$$

where the last integral is equal to

$$\int \frac{dk}{2\pi} \frac{\sin[knL]}{(k^2 + L_\omega^{-2})^2} = \frac{L_\omega n L}{4} \exp \left[-\frac{nL}{L_\omega} \right].$$

Then the current density can be rewritten as

$$j_H = \int_{-\infty}^{\infty} \frac{dE d\omega}{(2\pi)^2} f_E 8\pi\nu ev h_{E-\omega} \frac{D\tau}{l} \frac{\Lambda}{\nu D^2} \Im i \frac{2}{S} \sum_{n>0} \sin \left[2\pi n \frac{\Phi}{\Phi_0} \right] \frac{L_\omega n L}{4} \exp \left[-\frac{nL}{L_\omega} \right] =$$

$$= - \sum_{n>0} \sin \left[2\pi n \frac{\Phi}{\Phi_0} \right] \frac{4\pi e \Lambda n L}{D S} \Im i \int_{-\infty}^{\infty} \frac{dE}{2\pi} f_E \int_0^{\infty} \frac{d\omega}{2\pi} \left\{ h_{E-\omega} \frac{1+i}{\sqrt{2}} \sqrt{\frac{D}{\omega}} \times \right.$$

$$\left. \times \exp \left[-nL \frac{1-i}{\sqrt{2}} \sqrt{\frac{\omega}{D}} \right] + h_{E+\omega} \frac{1-i}{\sqrt{2}} \sqrt{\frac{D}{\omega}} \exp \left[-nL \frac{1+i}{\sqrt{2}} \sqrt{\frac{\omega}{D}} \right] \right\}. \quad (41)$$

The real part of curved brackets in (41) is equal to

$$\Re \{ \dots \} = \sqrt{\frac{D}{2\omega}} \exp \left[-\frac{nL}{\sqrt{2}} \sqrt{\frac{\omega}{D}} \right] (h_{E-\omega} + h_{E+\omega}) \left[\cos \left(\frac{nL}{\sqrt{2}} \sqrt{\frac{\omega}{D}} \right) - \sin \left(\frac{nL}{\sqrt{2}} \sqrt{\frac{\omega}{D}} \right) \right] =$$

$$= (h_{E-\omega} + h_{E+\omega}) \sqrt{\frac{D}{2\omega}} (\Re + \Im) \exp \left[-nL \frac{1+i}{\sqrt{2}} \sqrt{\frac{\omega}{D}} \right]. \quad (42)$$

In order to avoid the divergence of $\int dE$, we have to complete the coefficient of the diagram with terms that are equal to zero due to the analytic properties of the diagram. The divergence of $\int dE$ occurs due to the violation of the assumptions of the diffusion approximation. The completion the diagrams coefficient just provides the convergence of $\int dE$ on the values of $E \ll 1/\tau$, when the dependence of the Hikami box on E can be neglected.

In case of diagrams in Fig. 4, we can change their coefficient from $ih_{E-\omega}U_R(0)$ and $-ih_{E-\omega}U_R(\omega)/2$ to $i(h_{E-\omega} - 1)U_R(0)$ and $i(1 - h_{E-\omega})U_R(\omega)/2$. This will secure convergence of $\int dE$. As a consequence, in our expressions $\int dE f_E (h_{E-\omega} + h_{E+\omega})$ gets substituted with⁸

$$\frac{1}{2} \int dE [(1 - h_E h_{E-\omega}) + (1 - h_E h_{E+\omega}) + (h_{E-\omega} + h_{E+\omega} - 2h_E)] = 4\tilde{T}(\omega), \quad (43)$$

where $\tilde{T}(\omega)$ is defined as follows:

$$\tilde{T}(\omega) = \tilde{T}(-\omega) = \frac{1}{4} \int_{-\infty}^{\infty} dE (1 - h_E h_{E-\omega}). \quad (44)$$

where $\tilde{T} \equiv \tilde{T}(0)$ we call the effective temperature. In equilibrium $T(\omega) = \frac{\omega}{2} \coth \frac{\omega}{2T} \xrightarrow{\omega \rightarrow 0} T$, where T is the usual temperature.

⁸Eq. (43) becomes clear from (A84).

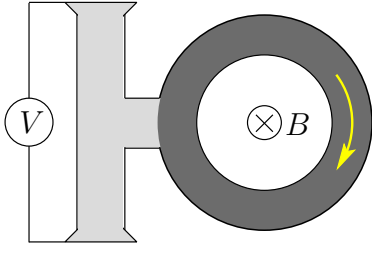


Figure 5: A way to sustain non-equilibrium steady state in a mesoscopic ring: an experimental installation.

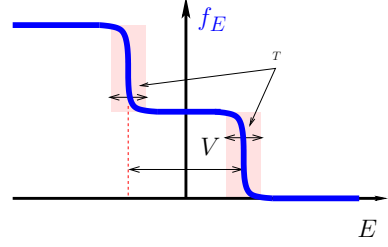


Figure 6: Simplified f_E dependence.

To obtain the net current, we multiply (41) by the ring's crosssection S :

$$I_H = j_H S = - \sum_{n>0} \sin \left[2\pi n \frac{\Phi}{\Phi_0} \right] \frac{8e\Lambda n L}{D} \int_0^\infty \frac{d\omega}{2\pi} \tilde{T}(\omega) \sqrt{\frac{D}{2\omega}} (\Re + \Im) \exp \left[-nL \frac{1+i}{\sqrt{2}} \sqrt{\frac{\omega}{D}} \right]. \quad (45)$$

Remembering the fact, that the contribution of the Fock diagram in Fig. 4(b) is twice smaller than that for the Hartree diagram (45) and comes with an opposite sign, we write the final result for the thermodynamic component of the net current along the ring:

$$I' = I_H/2 = \sum_{n>0} \sin \left[2\pi n \frac{\Phi}{\Phi_0} \right] I'_n, \\ I'_n = -\frac{4e\Lambda n L}{D} \int_0^\infty \frac{d\omega}{2\pi} \tilde{T}(\omega) \sqrt{\frac{D}{2\omega}} (\Re + \Im) \exp \left[-nL \frac{1+i}{\sqrt{2}} \sqrt{\frac{\omega}{D}} \right]. \quad (46)$$

Eq. (46) gives the current of electrons having arbitrary spin projection. Thus the net current is twice larger than the result (46). For similarity with [10], let us perform variable change $\omega \rightarrow z = L\sqrt{\frac{\omega}{2D}}$. Then we rewrite (46) as follows:

$$I'_n = -\frac{4e\Lambda n}{\pi} \int_0^\infty dz \tilde{T}(2z^2 E_T) (\Re + \Im) \exp[-nz(1+i)], \quad (47)$$

In equilibrium, at zero temperature, $\tilde{T}(\omega) = |\omega|/2$, and $I'_n = \frac{4eE_T\Lambda}{\pi n^2}$.

Let T be the smallest scale of function $\tilde{T}(\omega)$. In equilibrium T is the temperature. Then $\delta = \sqrt{T/E_T}$ is the smallest scale of function $\tilde{T}(2z^2 E_T)$ in (47). When δ is large, we can approximate $\tilde{T}(2z^2 E_T)$ with its expansion over z/δ hoping to obtain the asymptotic for the integral. However, these attempts fail because

$$\forall n \in \mathbb{N}, m \in \mathbb{N} \cup \{0\} \quad \int_0^\infty dz z^{4m} (\Re + \Im) \exp[-nz(1+i)] = 0.$$

We conclude that the asymptotic is non-analytic. As it was numerically shown in [10] for the equilibrium case, it is very similar to exponential.

Let us use model distribution function in Fig. 6 with

$$h_E = \frac{1}{2} \left[\tanh \frac{E+V/2}{2T} + \tanh \frac{E-V/2}{2T} \right]. \quad (48)$$

The corresponding $\tilde{T}(\omega)$ dependence is plotted in Fig. 7.

Consider the case when $T \ll E_T \ll V$. When $T \rightarrow 0$, the effective temperature \tilde{T} is equal to $V/4$, and

$$\tilde{T}(\omega) = \begin{cases} \frac{V+|\omega|}{4}, & |\omega| < V, \\ \frac{|\omega|}{2}, & |\omega| \geq V, \end{cases} \quad (49)$$

and the integral $\int dz$ in (47) can be divided into 2 parts:

$$I'_n = I_n^{(0)'} + I_n^{\tilde{T}'}, \quad I_n^{(0)'} \gg I_n^{\tilde{T}'}, \\ I_n^{(0)'} = -\frac{2eE_T\Lambda n}{\pi} \int_0^\infty dz z^2 (\Re + \Im) \exp[-nz(1+i)] = \frac{2eE_T\Lambda}{\pi n^2}, \\ I_n^{\tilde{T}'} = -\frac{2eE_T\Lambda n}{\pi} \int_{\sqrt{\frac{V}{2E_T}}}^\infty dz \left(z^2 - \frac{V}{2E_T} \right) (\Re + \Im) \exp[-nz(1+i)],$$

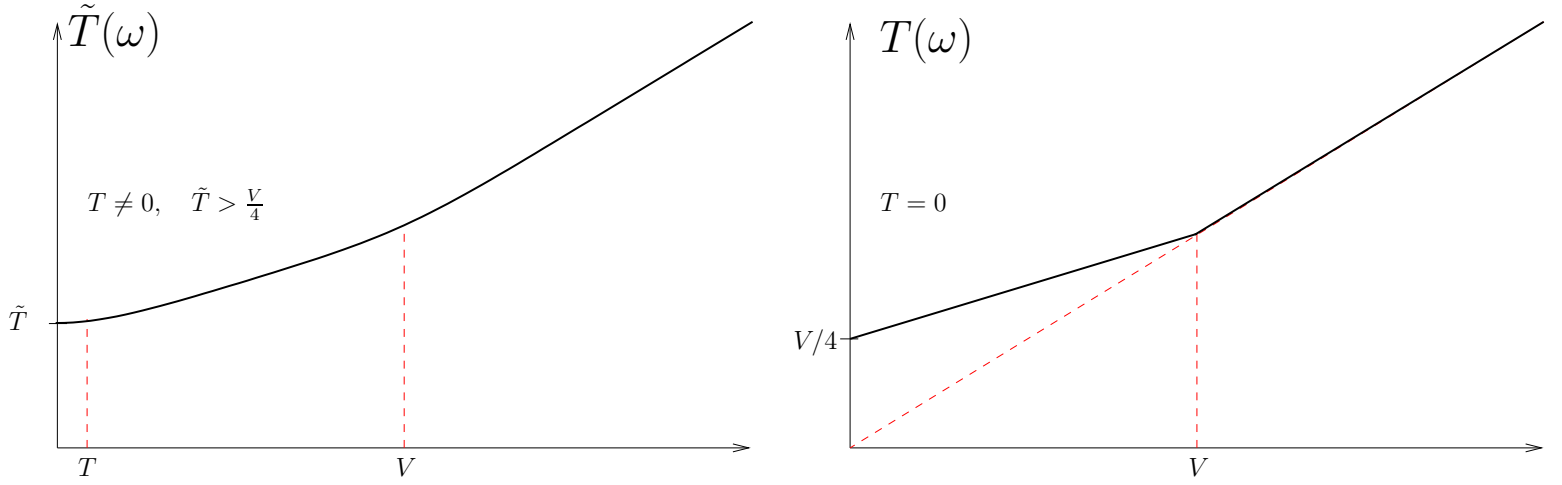


Figure 7: The frequency dependence of $\tilde{T}(\omega)$ for nonequilibrium energy distribution of the form (48). When $T = 0$, $\tilde{T}(\omega)$ is given by (49) (on the right).

so that the main contribution to the current is given by $I_n^{(0)'}$ which does not depend on the largest scale V of the distribution function. Thus we conclude that given $T \ll E_T \ll V$, the thermodynamic part of the persistent current remains finite no matter how much we increase V . This is the illustration of the fact that it is the smallest scale of the distribution function that governs the decay of the thermodynamic current. Here we have a separation of parameters analogous to what happens for the fluctuations of persistent current [15]: the largest scale \tilde{T} of the energy distribution function determines only the prefactor of a function depending on T/E_T .

3.2.2 The renormalization of the potential in the Cooper channel

The diagrams in Fig. 4 give origin to important series of diagrams shown in Fig. 8. Let us write the expression for the second term of

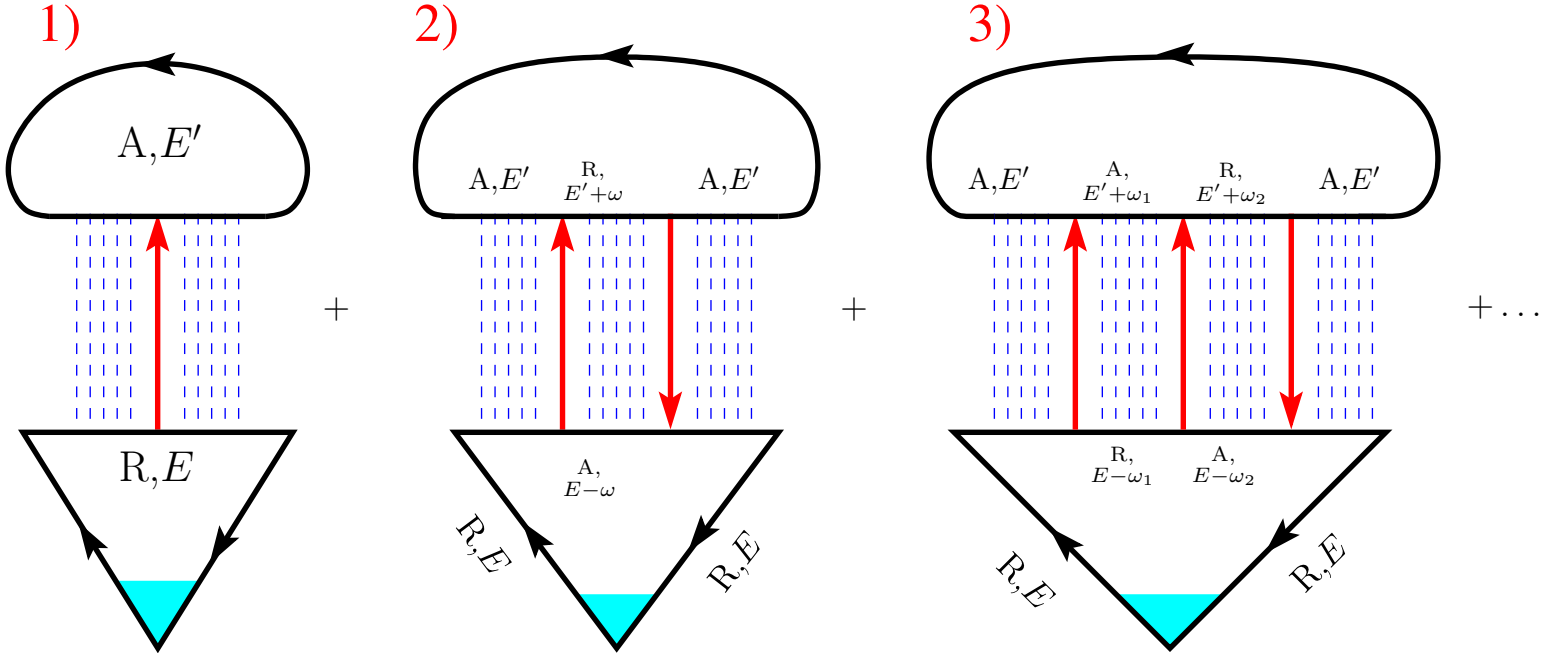


Figure 8: The renormalization in Cooper channel for the diagram in Fig. 4(a) (Hartree series). Bunches of dashed lines denote cooperons. The interaction lines are supposed to transfer large momentum $\sim p_F$, so that $U_{R/A} = \frac{\Lambda}{\nu}$ and $U_K = 0$. Here are the parts of coefficients of the diagrams providing the largest contribution: 1): $ih_{E'} \frac{\Lambda}{2\nu}$. 2): $\frac{1}{4}h_{E-\omega}h_{E'} \frac{\Lambda^2}{\nu^2}$. 3): $\frac{i}{8}h_{E'}h_{E'+\omega_1}h_{E-\omega_2} \frac{\Lambda^3}{\nu^3}$.

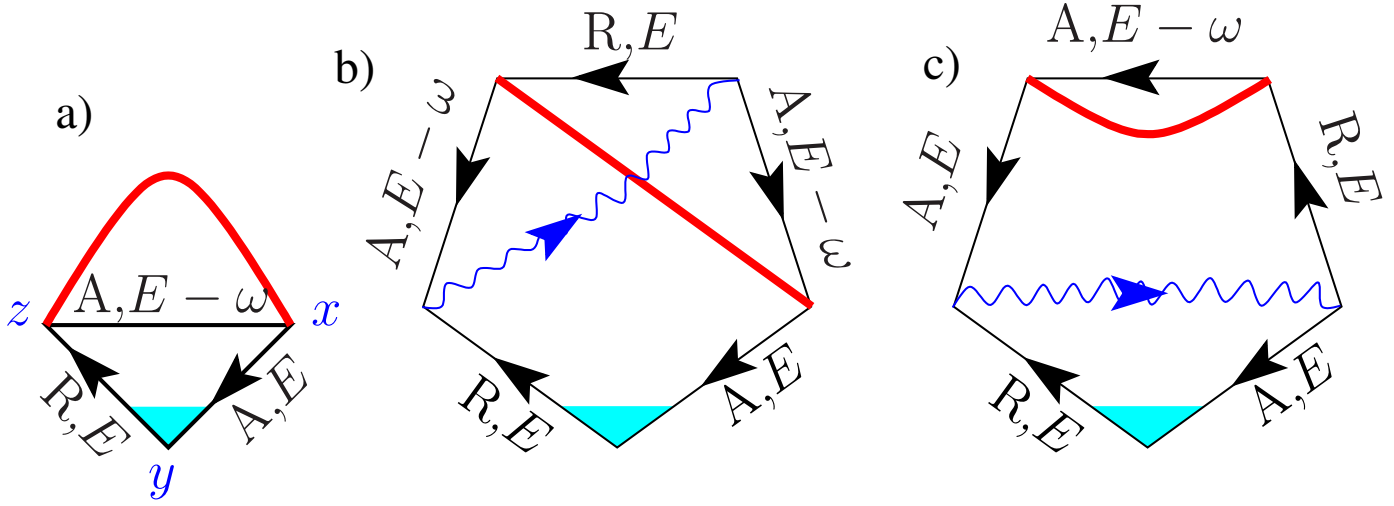


Figure 9: Diagrams for the current with the coefficient (53). For every diagram drawn here exists a complex-conjugated one with an opposite sign. a) “Initial” Fock diagram without cooperons and diffusons. b-c) Two first-loop diagrams.

the series, provided by the diagram in Fig. 8a2):

$$2iev \frac{(2\pi\nu\tau)^4}{(2\pi\nu\tau^2)^3} \int \frac{dE dE'}{(2\pi)^2} \frac{1}{V} \sum_{\vec{k}} \frac{-4\pi\nu D\tau^3 \vec{k}/l}{[Dk^2 - i(E - E')]^2} f_E \int \frac{d\omega}{2\pi} \frac{h_{E-\omega} h_{E'} \frac{\Lambda^2}{4\nu^2}}{Dk^2 - i(2\omega - E + E')}. \quad (50)$$

If in the last integral we can neglect Dk^2 and $E - E'$ with respect to ω , then the difference of (50) from (39) consists in the logarithmic factor:

$$-i \frac{(2\pi\nu\tau)^2}{2\pi\nu\tau^2} \frac{\Lambda}{2\nu} \int \frac{d\omega}{2\pi} \frac{h_{E-\omega}}{-2i\omega} = \frac{\Lambda}{4} \int d\omega \frac{h_{E-\omega}}{\omega} \approx -\frac{\Lambda}{2} \int_{\tilde{T}}^{E_F} \frac{d\omega}{|\omega|} = -\frac{\Lambda}{2} \log \frac{E_F}{\tilde{T}}, \quad (51)$$

where we used the fact that in a wide range of frequencies $\tilde{T} < |\omega| < E_F$, the integrand in (51) is proportional to $\frac{1}{|\omega|}$. Analogously, for $\tilde{T} < |\omega_{12}| < E_F$ the integrand in the expression for the diagram on fig. 83) is proportional to $\frac{1}{|\omega_1|} \frac{1}{|\omega_2|}$, which after integration, will result in the factor $\log^2 \frac{E_F}{\tilde{T}}$. Note that only diagrams drawn on fig. 8 have this property; other diagrams of second and third order in interaction with other combinations of $G_{R/A}$ are insignificant.

The series in Fig. 8 can be prolonged; every next diagram with an extra interaction line gains $\log \frac{E_F}{\tilde{T}}$, so that [6] instead of summing the entire series of diagrams in Fig. 8, one can take into account only diagrams in Fig. 4 with an interaction, “corrected” (or renormalized) by the factor

$$\frac{1}{1 + \frac{\Lambda}{2} \log \frac{E_F}{\tilde{T}}}. \quad (52)$$

This correction is called “the renormalization in the Cooper channel”⁹.

3.3 Kinetic part of persistent current

The first order of perturbation theory in interaction produces usual Hartree and Fock diagrams with expressions given by (32). Only Fock diagram gives non-zero contribution to the kinetic part of persistent current. One has to “dress” it with cooperon and diffuson lines in all possible ways selecting diagrams with the minimal number of loops. Diagrams with one loop are drawn in Fig. 9. Their coefficient

$$K = \frac{i}{2} \{ (h_E - h_{E-\omega}) U_K(\omega) - (1 - h_E h_{E-\omega}) [U_R(\omega) - U_A(\omega)] \}. \quad (53)$$

becomes small if the momentum transfered through the interaction line, is large.

Looking at fig. 9, we see that every pair of points in the first-loop diagrams b) and c) can be connected by a path consisting only of Green function lines. In coordinate space, Green functions (A10) decay exponentially: $G_{R/A}(\vec{r} - \vec{r}') \propto \exp \frac{|\vec{r} - \vec{r}'|}{l}$, where mean free path l is the smallest spatial scale of the disorder averaging technique. Thus diagrams b) and c) can be significant only when their interaction lines are short-range, or, in other words, when they carry large values of momentum $\gtrsim 1/l$. From here we conclude that first-loop diagrams b) and c) in Fig. 9 are insignificant, so that we have to explore the second-loop diagrams.

The calculations presented here were performed for the case of $E_T \ll T < \tilde{T}$. The deviations of the density of states ν_E from its value on Fermi level ν_0 were assumed to be small, $\nu_E - \nu_0 \ll \nu_0$. In the second loop most important diagrams can be divided in 3

⁹This section only illustrates, but does not prove the result (52). The proof is written in [6]; it requests using Dyson equation in terms of vertex parts [5].

groups each corresponding to one of three excitation channels [16]. At first we study the singlet channel which is represented by the diagram in Fig. 10 with a coefficient given by (53).

3.3.1 Singlet channel

Before we proceed with the calculations, let us make a note to section 3.1. There we discussed the division of a physical quantity into thermodynamic and kinetic parts. Two different ways to make this separation were suggested: (i) in terms of density matrix (27) and (ii) in terms of Keldysh component of matrix Green function (30). From (27) it is evident that only off-diagonal elements of an operator of a physical quantity enter into the expression for its kinetic part; if a quantity has diagonal operator, it has zero kinetic part.

We believe that the two definitions (27) and (30) are equivalent. If this is true, then if we substitute \hat{j} with any diagonal operator, we should get zero result for j'' calculated from the second definition (30). We can demonstrate this for the simplest case when \hat{j} gets substituted by unity operator: $\hat{j} \rightarrow \hat{1}$. After this substitution, let us use Lehman representation for $G_{R/A}$ on the ends of our diagram (before the averaging). Together with its complex-conjugated “sister”, the diagram in Fig. 9a) form expression (once the current operator is substituted with 1):

$$\int dx dy dz G_R(y, z; E) G_A(x, y; E) [G_R(z, x, E - \omega) - G_A(z, x, E - \omega)]. \quad (54)$$

One can see that

$$\int dy G_R(x, y) G_A(y, z) = \sum_{\lambda} \frac{\psi_{\lambda}^*(x) \psi_{\lambda}(z)}{(E - \epsilon_{\lambda})^2 + \delta^2} \propto G_R(x, z) - G_A(x, z),$$

so that (54) is proportional to

$$[G_R(z, x, E) - G_A(z, x, E)] [G_R(z, x, E - \omega) - G_A(z, x, E - \omega)].$$

The last expression is invariant to the transformation $\omega \rightarrow -\omega$, $E \rightarrow E - \omega$, while the diagram’s coefficient (53) changes sign, so that the result is zero.

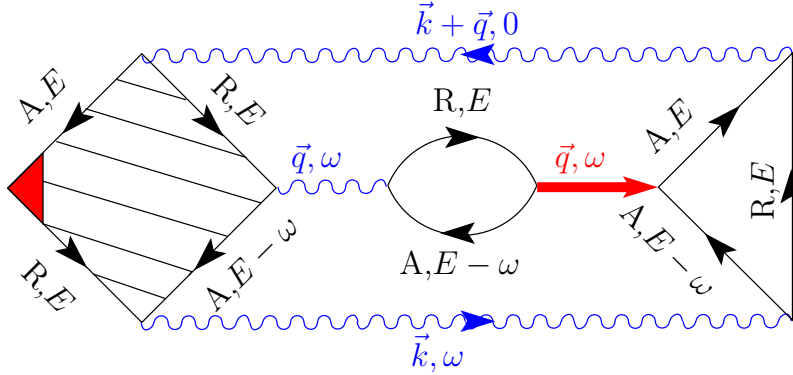


Figure 10: The simplest **singlet channel** diagram for the kinetic part of the current with a coefficient given by (53). Hikami box = $4\pi i \nu D \tau^4 \vec{q}/l$.

Let us now proceed with the calculation. First of all, let us evaluate the diagram’s coefficient (53). From (A48) it follows that in the universal limit (that is, when the screened interaction is independent on the original one)

$$U_{R/A} = \frac{\Pi_{A/R}}{\Pi_R \Pi_A}, \quad U_K = -\frac{\Pi_K}{\Pi_R \Pi_A}. \quad (55)$$

In expressions for the studied diagram, we have energy integrals by three variables: E , E' , and ω , where E' denotes the energy integration variable E from sec. 4.7. One can substitute (55) to (53), leaving the denominator evaluated without taking into account ν_E - dependence, and thus calculated using simple expressions (A58). This is due to the fact that $\Pi_R \Pi_A$ (see (A55)) is E and E' - independent, so that in expression for our diagram we can rearrange energy integrals in the manner

$$\int d\omega \frac{1}{\Pi_R \Pi_A} \int dE dE' R_{\omega}(E, E') \dots$$

If one neglects ν_E - dependence under $\int dE dE'$, $R_\omega(E, E')$ will rest the only quantity depending on E and E' ; then from (58) we see that $\int dE dE' R_\omega(E, E') = 0$. So we deduce that the correction to $\Pi_R \Pi_A$ in the denominator of (55), due to the dependence of $\nu_E \neq \text{const}$, lies out of the considered precession. With this argument, using (A55) and (A58), we get:

$$K = \frac{1}{2\nu_0 D_0 q^2} \int_{-\infty}^{\infty} dE' R_\omega(E, E') \frac{(D_0 q^2)^2 + \omega^2}{(D_{E'} q^2)^2 + \omega^2}, \quad (56)$$

$$R_\omega(E, E') = (h_E - h_{E-\omega})(1 - h_{E'} h_{E'-\omega}) - (h_{E'} - h_{E'-\omega})(1 - h_E h_{E-\omega}), \quad (57)$$

$$R_\omega(E, E') = -R_\omega(E', E), \quad R_{-\omega}(E' - \omega, E - \omega) = R_\omega(E, E') \quad (58)$$

The function $R_\omega(E, E')$ from (57) is the same as in the quantum kinetic equation [14], where it plays a role of a driving force guiding system to equilibrium. This is another illustration of the fact that the contribution we study is given exclusively by offdiagonal elements of both density matrix and current operator.

Using (A50), (A54) and (A65), we deduce that the contribution to the current from the diagram from fig. 10 is equal to

$$S \int_{-\infty}^{\infty} \frac{dE}{2\pi} \frac{d\omega}{2\pi} \frac{iev l_E}{2\nu_0 d D_0} \times \frac{1}{V} \sum_{\vec{m} \in \mathbb{Z}^d \setminus \{\vec{0}\}} \frac{\vec{q}_{\vec{m}}}{q_{\vec{m}}^2} \int_{-\infty}^{\infty} dE' R_\omega(E, E') \frac{(D_0 q_{\vec{m}}^2)^2 + \omega^2}{(D_{E'} q_{\vec{m}}^2)^2 + \omega^2} \times$$

$$\frac{1}{D_E q_{\vec{m}}^2 - i\omega} \times \frac{1}{V} \sum_{\vec{n} + \frac{\vec{\Phi}}{-\Phi_0} \in \mathbb{Z}^d} \frac{1}{D_E k_{\vec{n}}^2 - i\omega} \cdot \frac{1}{D_E (\vec{k}_{\vec{n}} + \vec{q}_{\vec{m}})^2} + \text{c.c.} \quad (59)$$

From (58) we see that (59) equals zero result, if the calculation is performed assuming $\nu = \text{const}$ ¹⁰. In order to obtain non-zero result, we thus have to take into account the energy dependence of the density of states.

Let us proceed with calculations for the case of thin quasi-one-dimensional ring. Using (A75), we notice that from both exponents $\exp[i \dots]$ that appear there, only their imaginary part $i \sin[\dots]$ survives, so that

$$j^{(S)} = - \sum_{n \geq 1} \sin \left[2\pi n \frac{\Phi}{-\Phi_0} \right] I_n^{(S)}, \quad (60)$$

$$I_n^{(S)} = - \int_{-\infty}^{\infty} \frac{dE}{2\pi} \frac{ev l_E}{\nu_0 d D_0} \int_{-\infty}^{\infty} \frac{d\omega}{2\pi} \int_{-\infty}^{\infty} dE' R_\omega(E, E') \times$$

$$\times 2\Im \frac{1}{L} \sum_{m \geq 1} \frac{1 - e^{-nL/L_\omega}}{(D_E q_m^2 - i\omega)^3} \cdot \frac{(D_0 q_m^2)^2 + \omega^2}{(D_{E'} q_m^2)^2 + \omega^2}, \quad (61)$$

where L_ω is defined in (40).

Consider the contribution of small $\omega \lesssim E_T \ll T$ to $\int d\omega$.

$$R_\omega(E, E') \approx \omega \left(\frac{\partial R_\omega(E, E')}{\partial \omega} \Big|_{\omega=0} \right). \quad (62)$$

As one can see from (63), the expansion of R in (62) over ω/T implies the expansion of the final result over E_T/T .

$$\Im \int_{-\infty}^{\infty} \frac{d\omega}{2\pi} \omega \frac{1 - e^{-nL/L_\omega}}{(D_E q_m^2 - i\omega)^3} \cdot \frac{D_0^2 q^4 + \omega^2}{D_{E'}^2 q^4 + \omega^2} =$$

$$\frac{D_0^2 - D_{E'}^2}{(D_E + D_{E'})^3} \times \frac{1 - e^{-nL|q| \sqrt{\frac{D_{E'}}{D_E}}}}{2q^2}. \quad (63)$$

In (63) we get zero in case of $D_0 = D_{E'}$; this means that in (61) we can neglect E -dependence of all the coefficients to the left from $\int_{-\infty}^{\infty} \frac{d\omega}{2\pi}$, because they will result in higher order corrections in $\delta\nu_E/\nu_E$; the same is true for the contribution of $\omega \gg E_T$ in the complex plane.

Let us define

$$C_n = \frac{6}{\pi^2} \sum_{m \geq 1} \frac{1 - \exp[-2\pi mn]}{m^2}, \quad n > 0, \quad C_\infty = 1. \quad (64)$$

$$I_n^{(S)} = C_n \frac{e}{48g} \int_{-\infty}^{\infty} \frac{dE dE'}{2\pi} \frac{\partial R_\omega(E, E')}{\partial \omega} \Big|_{\omega=0} \frac{\delta D_E}{D_0}, \quad g = \nu DS/L. \quad (65)$$

¹⁰so that, according to (A68), also $l_E = \text{const}$ and $D_E = \text{const}$.

Let us go ahead with the calculation, substituting in (65)

$$\begin{aligned} \left. \frac{\partial R_\omega(E, E')}{\partial \omega} \right|_{\omega=0} &= (1 - h_{E'}^2) h'_E - (\dots E \leftrightarrow E' \dots), \\ \left. \frac{\partial R_\epsilon(\delta E, \omega)}{\partial \delta E} \right|_{\delta E=0} &= \left(1 - h_{\epsilon + \frac{\omega}{2}}^2\right) h'_{\epsilon + \frac{\omega}{2}} - (\dots \omega \rightarrow -\omega \dots), \\ I_n^{(S)} &= -C_n \frac{e}{6g} \int_{-\infty}^{\infty} \frac{dE}{2\pi} \frac{\delta D_E}{D_0} \left[\frac{\tilde{T} h'_E}{2} - \frac{1 - h_E^2}{4} \right] = \frac{e}{6g\nu_0} \int_{-\infty}^{\infty} \frac{dE}{2\pi} \nu_E \left[\tilde{T} f'_E + f_E(1 - f_E) \right], \end{aligned} \quad (66)$$

where $f_E = (1 - h_E)/2$ is the energy distribution function.

3.3.2 Triplet channel

In section 3.3.1 at first glance it seems that all the diagrams beginning from the first order of the interaction were studied (the interaction line in Fig. 10 stands for complete RPA series). However, because the coefficient for the diagram in Fig. 10 approaches zero for the unscreened Coulomb interaction (for which $U_R = U_A$ and $U_K = 0$), the series of diagrams effectively start from the second order of the interaction. That is why one has to search for important dressed diagrams not only in the first but also in the second order of perturbation. In this way one finds out diagrams for triplet and superconducting channels, see fig. 12.

Let us first of all demonstrate that without taking $\nu(\xi)$ dependence into account the diagrams for superconducting and triplet channels give zero result (for singlet channel, this is done in sec. 3.3.1). Like the diagram for the singlet channel in Fig. 10, the coefficients of triplet and superconducting diagrams in Fig. 12 contain $R_\omega(E, E')$ defined in (57). It is convenient now to change variables from $\{E, E', \omega\}$ to $\{\epsilon, \delta E, \omega\}$, where $\delta E = E - E'$ and $\epsilon = \frac{E + E'}{2} - \omega$. In these new variables the coefficient $R_\epsilon(\delta E, \omega)$ (defined in (57)) is odd both in δE and ω :

$$R_\epsilon(\delta E, \omega) = \left(h_{\epsilon + \frac{\delta E + \omega}{2}} - h_{\epsilon + \frac{\delta E - \omega}{2}} \right) \left(1 - h_{\epsilon - \frac{\delta E + \omega}{2}} h_{\epsilon - \frac{\delta E - \omega}{2}} \right) - (\delta E \rightarrow -\delta E), \quad (67)$$

so that also the expression for the diagrams in Fig. 12 is to be antisymmetrized in δE and ω . In addition to that antisymmetrization, we must take $2\Im$ of the diagrams. For constant density of states $\nu(E) = \text{const}$ this is equivalent to the following operation: $[(\dots) - (\dots \omega \rightarrow -\omega, \delta E \rightarrow -\delta E \dots)]$. Together with antisymmetric properties of (67) this leads to conclusion that triplet and Cooper diagrams = 0 in case of constant density of states. This statement is still true if diffusion coefficients depend only on ϵ .

In our energy integrals, energy variables can be confined by three energy scales: $E_T \sim 10\text{mK}$ or $\tilde{T} \gg T \gg E_T$. Let us name an energy variable “small” if its integral converges on the values of $\lesssim E_T$, and large otherwise. If a variable is small, it has to enter into frequencies of cooperons and/or diffusons; otherwise only the temperature coefficient R of a diagram can provide convergence, and the considered energy variable is condemned to be large (because R , given by (67), does not depend on E_T).

With this reasoning we conclude that ϵ is surely a large variable, because diffusons and cooperons do not have poles on it. Thus the integration area where both $\delta E, \omega \ll \tilde{T}$ give zero contribution to the result (because in this case $\delta E, \omega \ll \epsilon \lesssim T$ or even $\epsilon \lesssim \tilde{T}$, so that $D_{\epsilon \pm \delta E} \approx D_{\epsilon \pm \omega} \approx D_\epsilon$).

Superconducting diagrams from fig. 12 are estimated as $(E_T/T)^2$ smaller then those from the triplet channel. Moreover, the superconducting channel fig. 12(b) acquires additional smallness due to the renormalization of the potential in the Cooper channel (see sec. 3.2.2).

The contribution of the triplet channel to the current is equal to

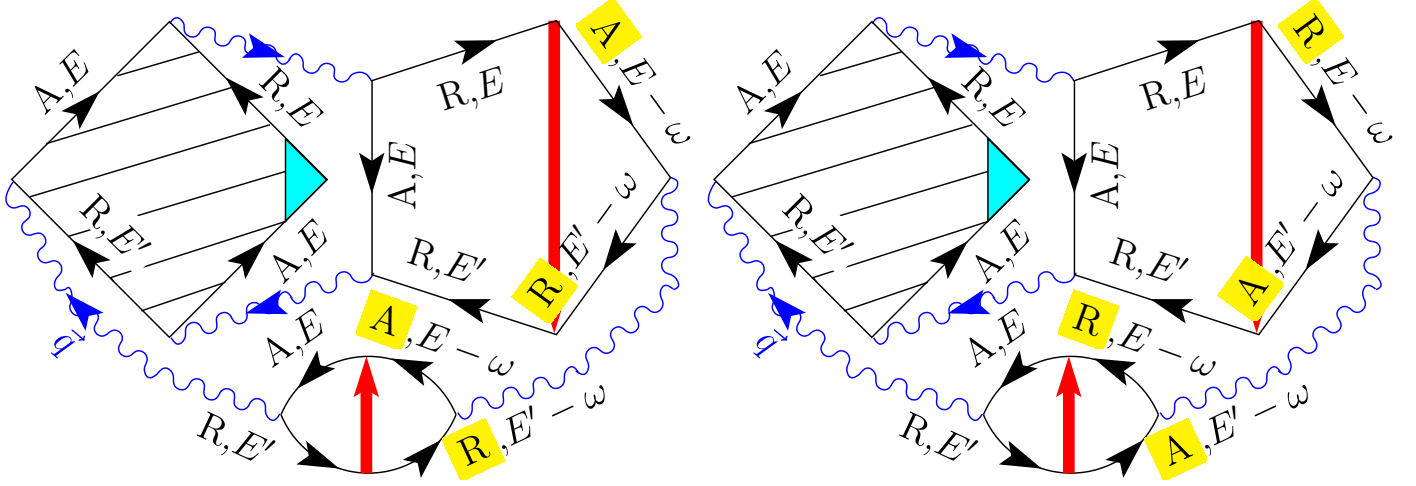
$$\begin{aligned} I &= S \frac{1}{V} \sum_q \int \frac{dE dE' d\omega}{(2\pi)^3} 2\Re(-2\pi i e \nu_{E-\omega} D_E q) \frac{\Lambda^2}{\nu_0^2} \times \\ &\times \frac{1}{D_E q^2 + i\delta E} \left[\frac{1}{D_{E-\omega} q^2 + i\delta E} + \text{c.c.} \right] \times \frac{1}{V} \sum_{k'} \frac{1}{D_E^2 (k+q)^2} \frac{1}{k^2 + L_{\delta E}^{-2}}, \end{aligned}$$

where $L_{\delta E} = \sqrt{D_E/(i\delta E)}$, $\Re L_{\delta E}$ (see (40)). The sum $\frac{1}{V} \sum_{k'}$ is given by (71) with ω changed to $-\delta E$, so that we can write our current in a usual form (60) with harmonics given by

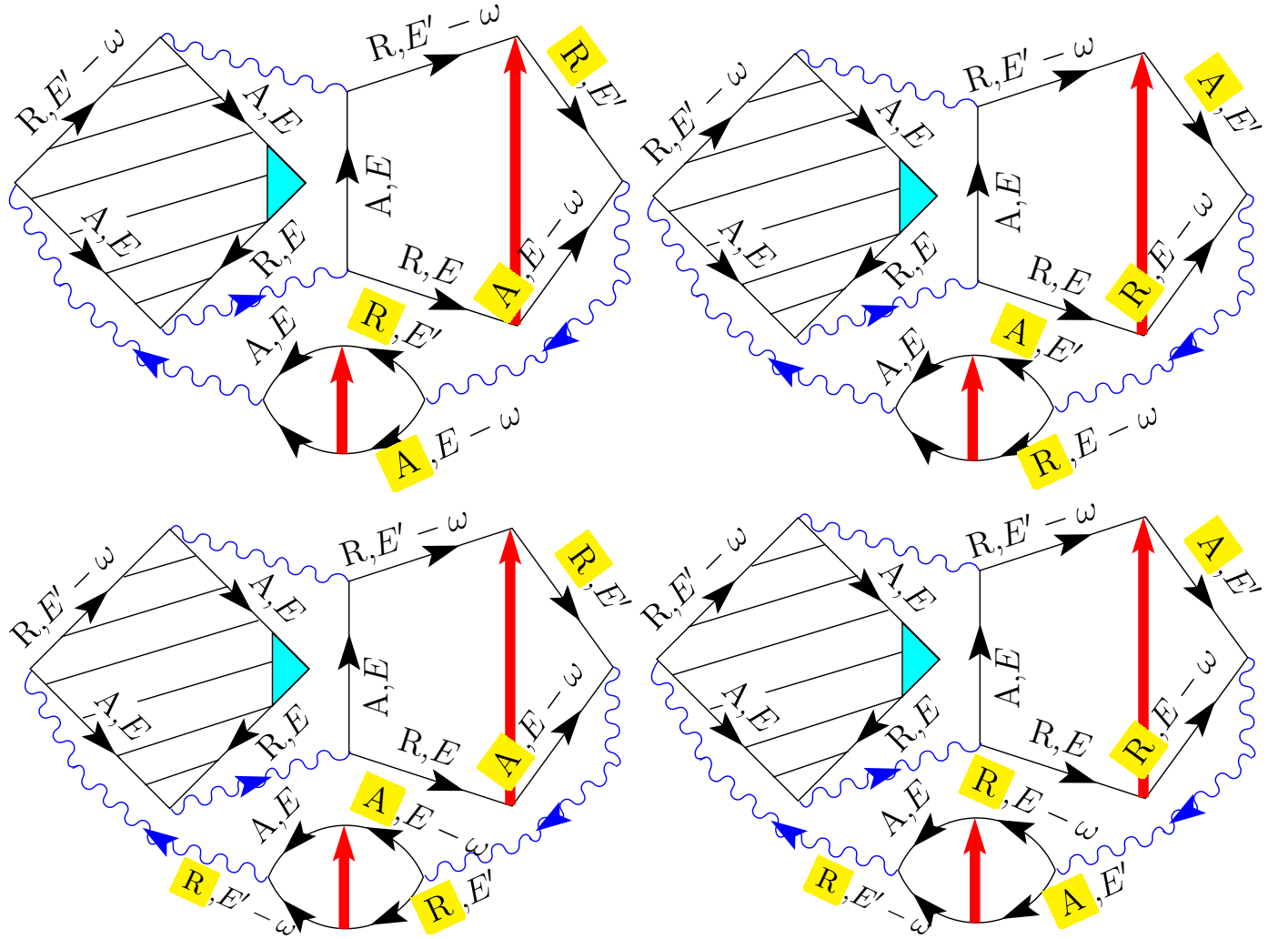
$$I_n^{(T)} = \frac{4}{V} \sum_{q>0} \int \frac{d\epsilon d\omega}{2\pi} e \nu_0 \frac{\Lambda^2}{\nu_0^2} \Im \int \frac{d\delta E}{2\pi} R_\epsilon(\delta E, \omega) \frac{D_0 D_E q^4}{(D_{E-\omega} q^2)^2 + \delta E^2} \frac{1 - \exp[-nL/L_{\delta E}]}{(D_E q^2 + i\delta E)^3}, \quad (68)$$

We close the integration path, avoiding crossing the branchcut (see fig. 14), and the result is given, as usually, by the poles in the region $-\frac{\pi}{2} < \arg i\delta E < \frac{\pi}{2}$. Since $\exp[-2\pi] < 0.002$, we neglect the exponential term in (68):

$$\Im \int \frac{d\delta E}{2\pi} \dots = \frac{D_0 D_E}{2(D_E + D_{E-\omega})^3} \cdot \frac{L^2}{18(2\pi)^2} \cdot \frac{\pi^2}{6} \left(\left. \frac{\partial R_\epsilon(\delta E, \omega)}{\partial \delta E} \right|_{\delta E=0} \right),$$



(a) Triplet channel.



(b) Cooper channel.

Figure 12: Simplest diagrams for triplet and superconducting channels. Every diagram has in addition its complex conjugated pair with an opposite sign, so one should take twice imaginary part. Dashed square represents Hikami box with a current vertex; interaction is drawn with a thick straight line; wavy lines stand for cooperons and diffusons. All diagrams here have coefficient $\frac{\Delta^2}{v_0^2} R_\omega(E, E')$ with $R_\omega(E, E')$ defined in (57).

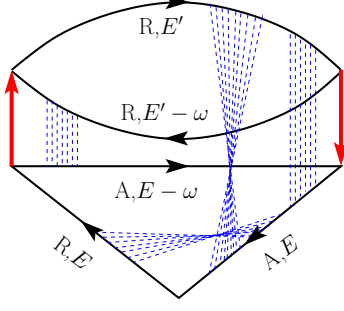


Figure 13: The first diagram from fig. 12(a).

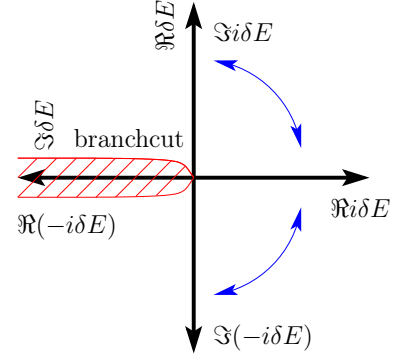


Figure 14: $\int d\delta E$ in complex plane.

$$I_n^{(T)} = \frac{e\Lambda^2 D_0^2}{6g} \int \frac{d\epsilon d\omega}{2\pi} \frac{D_E}{2(D_E + D_{E-\omega})^3} \left(\frac{\partial R_\epsilon(\delta E, \omega)}{\partial \delta E} \Big|_{\delta E=0} \right).$$

Then let us substitute $E = \epsilon + \frac{\omega}{2} + \frac{\delta E}{2} \approx \epsilon + \frac{\omega}{2}$ and $E - \omega \approx \epsilon - \frac{\omega}{2}$. This approximation is valid because the region $\{\delta E, \omega | \delta E, \omega \lesssim E_T \ll T\}$ is negligibly small in our whole integration space so that we can drop δE from the expressions for E and $E - \omega$. Then we perform variable change: $\epsilon + \frac{\omega}{2} \rightarrow E$, $\epsilon - \frac{\omega}{2} \rightarrow E'$. Expanding $\frac{D_E}{2(D_E + D_{E-\omega})^3}$ and antisymmetrizing it by ω , we get $-\frac{\delta D_E - \delta D_{E'}}{16D_0^3}$ instead, so that

$$I_n^{(T)} = -\frac{e\Lambda^2}{48g} \int \frac{dE dE'}{2\pi} \frac{\delta D_E}{D_0} \left(\frac{\partial R_\omega(E, E')}{\partial \omega} \Big|_{\omega=0} \right) = \frac{e\Lambda^2}{6g\nu_0} \int \frac{dE}{2\pi} \nu_E \left[\frac{\tilde{T}h'_E}{2} - \frac{1 - h_E^2}{4} \right] \quad (69)$$

Taking spin into account leads to triplication of the result (69), see [16]. The second part of (69) has the same structure as singlet channel (65); however, it has different sign. In case of short range potential (69) is cancelled by (72), and this is the manifestation of the fact that short range interaction gives zero effect for fermions if one does not take spin into account, see sec. 3.3.3.

3.3.3 Singlet channel in case of a $\delta(\vec{r} - \vec{r}')$ -like interaction

The aim of this subsection is to control that singlet and triplet channels are calculated correctly and no contributions of the same order are missing.

Let us see how calculation of the singlet channel contribution changes for a point-like interaction. In case of spinless fermions, the result should cancel that of the triplet channel. This is because $\delta(\vec{r} - \vec{r}')$ -like interaction term is proportional to $\psi^\dagger(\vec{r})\psi^\dagger(\vec{r})\psi(\vec{r})\psi(\vec{r}) = 0$ for spinless fermions.

One could observe it in section 3.2 for the thermodynamic part of persistent current; let us check that this happens also for its kinetic part. The expression for the triplet channel would be the same as in the case of Coulomb interaction, see sec. 3.3.2. The result for the singlet channel will be different.

While even for the case of weak Coulomb interaction the RPA renormalization (see sec. 4.7) is important because of its long-range nature, for point interaction it is enough to calculate the coefficient (53) in the first non-vanishing order of the RPA-sequence. In the momentum space, the bare interaction is just a constant

$$U^{(0)}(\vec{q}, \omega) = \frac{\Lambda}{\nu_0}, \quad \Lambda \ll 1, \quad (70)$$

which, once being substituted into (53), produces zero result. Then we calculate the second order term in the RPA series (see fig. 19), using (70) as an expression for a bare interaction line:

$$U(\vec{q}, \omega) = \frac{\Lambda^2}{\nu_0^2} \Pi(\vec{q}, \omega),$$

where $\Pi(\vec{q}, \omega)$ is given by (A50), (A51), and (A52). This time we get non zero result from (53):

$$K = \frac{\Lambda^2 \tau_0}{4\nu_0} \int dE' R_\omega(E, E') \left[\frac{X}{1-X} + \frac{X^*}{1-X^*} \right] = \frac{\Lambda^2}{2\nu_0} \int dE' R_\omega(E, E') \frac{D_0 q^2}{(D_{E'} q^2)^2 + \omega^2}.$$

The expression for the current is as follows:

$$\vec{I} = S \frac{1}{V} \sum_q \int \frac{dE dE' d\omega}{(2\pi)^2} 2\Re i D_E \vec{q} \cdot K \cdot \frac{1}{D_E q^2 - i\omega} \frac{1}{V} \sum_{k'} \frac{1}{D_E^2 (k+q)^2} \frac{1}{k^2 + L_\omega^{-2}},$$

$$\frac{1}{V} \sum_{k'} = -\frac{2}{S} \sum_{n>0} \sin \left[2\pi n \frac{\Phi}{-\Phi_0} \right] q \frac{1 - \exp[-nL/L_\omega]}{(D_E q^2 - i\omega)^2}, \quad (71)$$

so that

$$\begin{aligned} I &= - \sum_{n>0} \sin \left[2\pi n \frac{\Phi}{-\Phi_0} \right] I_n^{(S)}, \quad I_n^{(S)} = - \int \frac{dE dE'}{2\pi} 4e \frac{\Lambda^2}{\nu_0} \times \\ &\times \frac{1}{V} \sum_{q>0} \Im \int \frac{d\omega}{2\pi} R_\omega(E, E') \frac{D_0 D_E q^4}{(D_{E'} q^2)^2 + \omega^2} \frac{1 - \exp[-nL/L_\omega]}{(D_E q^2 - i\omega)^3}. \\ \Im \int \frac{d\omega}{2\pi} \dots &= \left(\frac{\partial R_\omega(E, E')}{\partial \omega} \Big|_{\omega=0} \right) \frac{D_0 D_E}{(D_{E'} + D_E)^3} \frac{1 - \exp \left[-2\pi m n \sqrt{\frac{D_{E'}}{D_E}} \right]}{2(2\pi m/L)^2}, \end{aligned}$$

Expanding $\frac{D_E}{2(D_E + D_{E'})^3}$ and antisymmetrizing it by ω , we get $-\frac{\delta D_E - \delta D_{E'}}{16D_0^3}$ instead.

$$\begin{aligned} I_n^{(S)} &= -\frac{e\Lambda^2}{12g} \int \frac{dE dE'}{2\pi} \left(\frac{\partial R_\omega(E, E')}{\partial \omega} \Big|_{\omega=0} \right) \frac{D_0^2 D_E}{(D_E + D_{E'})^3} C_n = \\ &= -\Lambda^2 \frac{e}{6g\nu_0} \int \frac{dE}{2\pi} \nu_E \left[\frac{\tilde{T} h'_E}{2} - \frac{1 - h_E^2}{4} \right]. \end{aligned} \quad (72)$$

One can see that it really cancels the contribution of the triplet channel calculated in section 3.3.2.

3.4 Result and its discussion

Out of equilibrium, the average of persistent in a mesoscopic ring is given by the thermodynamic and kinetic contributions. Given that the smallest scale T of the energy distribution function is much larger than the Thouless energy, $E_T \ll T$, the entire current is given by expressions (46), (65), and (69):

$$I = \sum_{n \geq 1} \sin \left[2\pi n \frac{\Phi}{\Phi_0} \right] I_n, \quad I_n = I'_n + I''_n, \quad (73)$$

$$\begin{aligned} I'_n &= -\frac{8e\Lambda nL}{D} \int_0^\infty \frac{d\omega}{2\pi} \tilde{T}(\omega) \sqrt{\frac{D}{2\omega}} (\Re + \Im) \exp \left[-nL \frac{1+i}{\sqrt{2}} \sqrt{\frac{\omega}{D}} \right], \\ I''_n &= I_n^{(S)} + I_n^{(T)} = -(1 - 3\Lambda^2) \frac{e\tilde{T}}{6g} \int_{-\infty}^\infty \frac{dE}{2\pi} \left(\frac{D_E}{D_0} \right) \left[\frac{f_E(1 - f_E)}{\tilde{T}} + \frac{\partial f_E}{\partial E} \right], \end{aligned} \quad (74)$$

where f_E is the energy distribution function, D_E is the energy-dependent diffusion coefficient, $\tilde{T}(\omega) = \frac{1}{4} \int_{-\infty}^\infty dE (1 - h_E h_{E-\omega})$, $\tilde{T} \equiv \tilde{T}(0) = \int dE f_E (1 - f_E)$ is the effective temperature, and $g = \nu D S / L$ is the dimensionless conductance, $\Lambda \ll 1$ is the constant characterizing interaction strength on short distances, see (A56).

Note that $f_E(1 - f_E) = \overline{(\delta n_E)^2}$ is equal to the average thermal fluctuation of the occupation number of arbitrary state that has an energy E .

While in equilibrium two terms in the square brackets of (74) cancel each other for any fixed energy E , in a non-equilibrium steady state with constant density of states this cancellation occurs after integrating over energy. Thus in case of constant density of states $I''_n = 0$.

Note that the effect studied is not due to the breaking of particle-hole symmetry (unlike in case of thermoelectric/acoustic effects and Coulomb drag). Indeed, suppose our nonequilibrium energy distribution has particle-hole symmetry, $h_E = -h_{-E}$. However, breaking it with an energy-dependence of the density of states $\nu_E = \nu_0 + \nu'_0 E$ is not enough – the result (74) will be zero. The reason is that, in addition to the particle conservation law, $\int St[E] dE = 0$ there is also conservation of energy: $\int St[E] E dE = 0$.

Unlike the thermodynamical current [10], the expression (74) for I''_n is not strongly suppressed if $E_T \ll T$. The decay of I''_n is governed by dephasing $\exp[-L/L_\phi]$, where L_ϕ is the coherence length. In the considered quasi-one-dimensional case $L/L_\phi = (\tilde{T}/gE_T)^{1/2}$, see sec. 4.3.

In Fig. 15 a) we propose an experiment that could permit measuring j'' . Non-equilibrium energy distribution in the ring is obtained by using metallic strip placed between two electrodes under voltage V . The energy distribution f_E and diffusion coefficient energy dependence D_E in the strip are shown on fig. 16, see ref. [17]. Given the strip short and thick enough, one can ignore interaction effects in it, supposing its density matrix to be diagonal. Attached to a mesoscopic ring, the strip can be considered as a “non-equilibrium reservoir” that exports f_E into the ring, where the interaction produces off-diagonal matrix elements. Note that during the calculation we have neglected the effects due to the inhomogeneity of f_E in the ring. The area of the contact connecting the strip with the ring should be much smaller than the ring’s crosssection; otherwise the exchange of electrons between the ring and the strip would compromise the coherence in the ring.

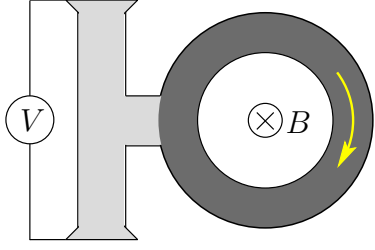


Figure 15: A way to sustain non-equilibrium steady state in a mesoscopic ring: an experimental installation.

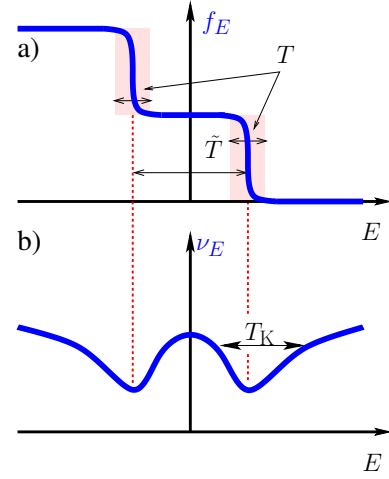


Figure 16: Simplified f_E and D_E dependences.

3.5 Discussion

We have calculated kinetic part of the current I''_n for $E_T \ll T$. In such conditions, the thermodynamic part of the current is very (almost exponentially) small (see sec. 3.2), and the persistent current is represented entirely by its kinetic component (74).

Using simplified f_E and D_E dependences from fig. 16, we estimate (74) as:

$$I_1 \sim (1 - 3\Lambda^2) \frac{e\Delta}{g} \frac{\delta D}{D} \times \begin{cases} (\tilde{T}/\Delta)^3, \tilde{T} \ll \Delta, \\ -\tilde{T}/\Delta, \tilde{T} \gg \Delta, \end{cases} \quad (75)$$

where $\frac{\delta D}{D}$ is the characteristic relative deviation of the diffusion coefficient. In (75), the asymptotic for $\tilde{T} \gg \Delta$ is universal, while the one for $\tilde{T} \ll \Delta$ was calculated for the Lorentzian D_E dependence.

Suppose $D_E \neq \text{const}$ due to the Kondo effect [18]; then the width Δ of the dips in D_E dependence is of the order of Kondo temperature T_K . Moreover, the effect vanishes for $\tilde{T} \gtrsim \Delta \sim T_K$ because of the rapid decay of $\frac{\delta D}{D}$. Thus from (75) it follows that its maximal value I''_n has at $\tilde{T} \sim \delta \sim T_K$. The approximate temperature dependence of I''_n is sketched in Fig. 17.

Let us estimate the result (74), assuming that $T = T_K$ so that the scattering crosssection of a Kondo impurity approaches λ_F^2 . Then the mean free path of an electron has two contributions: the usual one $1/l_0 = n\sigma_0$ and the contribution due to the Kondo effect: $\delta(1/l) = n_K \lambda_F^2$, where n and n_K are concentrations of normal and magnetic impurities:

$$\frac{1}{l} = n\sigma_0 + n_K \lambda_F^2, \quad n_K \ll n_0. \quad (76)$$

From (76) we estimate

$$\frac{\delta D}{D} \sim \frac{\delta l}{l} \sim n_K \lambda_F^2 l = \frac{n_K}{n_0} \frac{l}{\lambda_F}, \quad (77)$$

where $n_0 = \lambda_F^{-3}$ is a concentration of electrons which we estimate as a concentration of atoms.

A typical voltage in experiments is $10^{-3}V$; it corresponds to temperature $\sim 10K$. A typical size of a ring $L \sim 10\mu m$, Thouless energy $E_T \sim 10mK$, mean free path of an electron $l \sim 100\lambda_F$. Then the kinetic part of persistent current is of the order of

$$I_1 \sim \frac{e}{g} \left(\frac{eV}{h} \right) \frac{\delta D}{D} \quad (78)$$

If the concentration of magnetic impurities is high, $n_K/n_0 \sim 10^{-3} = 1000\text{ppm}$, from (77) and (78) we estimate $I \sim 0.1nA$.

In the considered situation, when $E_T \ll T$, I''_n is much larger than the thermodynamic component I'_n . Thus one can say that two components of persistent current are separated: the thermodynamic component I'_n rules for small $T \lesssim E_T$, while for $T \gg E_T$, the kinetic component I''_n becomes the most important. Let us now compare the value of I'_n for $T = 0$ with the value of I''_n for $E_T \ll T < \tilde{T} \sim T_K$. Without taking into account the renormalization in the Cooper channel (see sec. 3.2.2), the thermodynamic component of persistent current is of the order of $\sim 0.1nA$. The renormalization in the Cooper channel diminishes this value by the factor of $\log^{-1} \left(\frac{E_F}{\max(T, E_T)} \right) \sim 12$. Thus the maximal values of thermodynamic and kinetic parts of persistent current become equal when concentration of magnetic impurities equals $\sim 100\text{ppm}$.

3.6 Conclusions

In this section we studied the behaviour of persistent current in a system of many mesoscopic quasi-onedimensional rings in a non-equilibrium steady state. Out of equilibrium, in addition to the usual thermodynamic term I' , another, kinetic term I'' contributes to the persistent current. The manifestation of I'' occurs only if the density of states is energy dependent.

The temperature dependence of I' is governed exclusively by the smallest scale T of the energy distribution function f_E . It is independent of other scales of f_E if they are much larger than T .

On the contrary, given that $E_T \ll T$, I'' is insensitive to T and is governed primarily by the largest scale \tilde{T} of f_E .

There is a sort of separation between the two components on temperature scale: each of the two, I' and I'' give major contribution to the persistent for different ranges of values of T .

In addition, I' can be eliminated by application of strong parallel magnetic field.

We wish to thank for fruitful discussions Igor Aleiner, Boris Narozhny, and Igor Lerner.

4 Appendix

4.1 Trace of a thermodynamic current operator

Let us demonstrate that in (2) $f_T(E)$ can be shifted by an arbitrary constant [19]. In other words, trace of thermodynamic part of a current operator¹¹ equals zero:

$$\langle \vec{r}, E | \hat{j} | \vec{r}', E' \rangle = \frac{e}{2m} (\vec{\nabla}_{\vec{r}} - \vec{\nabla}_{\vec{r}'} - 2ie\vec{A}) [G_R(\vec{r}, \vec{r}'; E, E') - G_A(\vec{r}, \vec{r}'; E, E')], \quad (\text{A1})$$

$$\forall \vec{r} \quad \int dE \langle \vec{r}, E | \hat{j} | \vec{r}, E \rangle = 0, \quad (\text{A2})$$

where $G_{R/A}(\vec{r}, \vec{r}'; E, E')$ are Fourier transformations of Green functions (A79) in both time variables.

In a non-interacting system current is given by thermodynamic formula:

$$\vec{j}(\vec{r}) = -\frac{\delta \bar{E}}{\delta \vec{A}(\vec{r})}, \quad \bar{E} = \int_{-E_F}^{\infty} dE \nu_E f_T(E) E = \sum_n f_T(E_n) E_n. \quad (\text{A3})$$

From (2) and (A3) we conclude that

$$\vec{j}(\vec{r}, E_n) = -\frac{\delta E_n}{\delta \vec{A}(\vec{r})}$$


We have to prove that $\sum_n \vec{j}(\vec{r}, E_n) = 0$. Due to the known theorem from thermodynamics [20], a derivative of the average by the variable representing an external force is equal to the average from the derivative of an operator by this variable. and thus

$$\sum_n \vec{j}(\vec{r}, E_n) = -\sum_n \left\langle n \left| \frac{\delta \hat{H}}{\delta \vec{A}(\vec{r})} \right| n \right\rangle = -\frac{\delta}{\delta \vec{A}(\vec{r})} \text{Sp} \left[\hat{H} - \hat{H} \Big|_{\vec{A}=0} \right], \quad (\text{A4})$$

where in the right part of the expression we subtracted Hamiltonian of the system without magnetic field, in order to preserve convergence of Sp. In coordinate representation the dependence of the Hamiltonian on vector potential is given by $\hat{H}(\vec{r}, \vec{r}') = \hat{H}(\vec{r}, \vec{r}') \Big|_{\vec{A}=0} \exp[ie\vec{A}(\vec{r} - \vec{r}')]$, so that its diagonal matrix elements do not depend on \vec{A} , and (A4) equals zero.

In section 2 this permits us to substitute Fermi distribution function (2) with $-\frac{1}{2} \tanh \frac{E}{2T}$.

The statement (A2) is true also for thermodynamic part of the current in a non-equilibrium system with interaction: that's because any interaction corrections to the the diagonal part of the current operator (A1) gives zero contribution to (A2) due to their analytic properties.

 **Later (06.03.2006) note:** in other words, we have demonstrated that $\text{Sp} \hat{j} = 0$. From pp. [21]283-284 we know that the part of the current operator expanded in the powers of \hat{H} (where \hat{H} is the *unperturbed* Hamiltonian) can not give any contribution to the linear response, so that without the loss of generality it is zero:

$$\forall n \geq 0 \quad \frac{\text{Sp}[\hat{H}^n \hat{j}]}{\text{Sp} \hat{H}} \hat{H}^n = 0.$$

4.2 Density matrix in quasiequilibrium state

Consider a nonequilibrium system where energy distribution¹² relaxes to equilibrium much slower than the rest of physical quantities characterizing the system. Then in a certain range of time scales we can approximate complete density matrix of the system with the density matrix having maximal entropy with a fixed energy distribution. In [21], the physical state described by such a matrix is called quasiequilibrium state.

In this section we demonstrate that one-particle quasiequilibrium density matrix is diagonal. Let Λ denote the entire set of quantum numbers characterizing the state of a many-electron system in a representation with the diagonal Hamiltonian (including its part responsible for the interaction). We have to find conditional extremum of the entropy

$$\sigma = -\sum_{\Lambda} \rho_{\Lambda\Lambda} \log \rho_{\Lambda\Lambda}, \quad (\text{A5})$$

with additional conditions:

$$\text{Sp} \hat{\rho} = 1, \quad \text{Sp} \left[\hat{\rho} \delta(E - \hat{H}) \right] = f_E. \quad (\text{A6})$$

¹¹See sec. 3.1 for the definition.

¹²See [21] for the discussion about more general case.

where f_E stands for given energy distribution function. The first condition in (A6) corresponds to one Lagrange multiplier $\Phi - 1$, while the second one - to the set $\{F_E\}$:

$$\delta \left\{ -\text{Sp} \hat{\rho} \log \hat{\rho} - (\Phi - 1) \text{Sp} \hat{\rho} - \int dE F_E \text{Sp} [\hat{\rho} \delta(E - \hat{H})] \right\} = 0.$$

From (A5) one deduces that [21] $\delta\sigma = -\text{Sp} [(1 + \log \hat{\rho}) \delta \hat{\rho}]$, so that *complete* quasiequilibrium density matrix is given by

$$\hat{\rho} = \exp \left[-\Phi - \int dE F_E \delta(E - \hat{H}) \right], \quad (\text{A7})$$

which is certainly diagonal in the Λ -representation we have chosen (since the Hamiltonian is diagonal). Lagrange multipliers are determined from conditions

$$\begin{aligned} \sum_{\Lambda} \langle \Lambda | \exp \left[-\Phi - \int dE F_E \text{Sp} [\hat{\rho} \delta(E - \epsilon_{\Lambda})] \right] | \Lambda \rangle &= 1, \\ \sum_{\Lambda} \langle \Lambda | \exp \left[-\Phi - \int dE' F_{E'} \text{Sp} [\hat{\rho} \delta(E' - \epsilon_{\Lambda})] \right] \delta(E - \epsilon_{\Lambda}) | \Lambda \rangle &= f_E, \end{aligned}$$

Now let degrade complete density matrix (A7) to the one particle one. Let $|\lambda\rangle$ denote one-particle state, $\langle \lambda | \lambda' \rangle = \delta_{\lambda\lambda'}$. One particle density matrix is given by [22]

$$\rho_{\lambda\lambda'} = \langle a_{\lambda}^{\dagger} a_{\lambda'} \rangle = \sum_{\Lambda} \exp \left[-\Phi - \int dE' F_{E'} \delta(E' - \epsilon_{\Lambda}) \right] \langle \Lambda | a_{\lambda}^{\dagger} a_{\lambda'} | \Lambda \rangle$$

Given $\langle \Lambda | \Lambda' \rangle \propto \delta_{\Lambda\Lambda'}$, one concludes that quasiequilibrium one-particle density matrix is diagonal: $\rho_{\lambda\lambda'} \propto \delta_{\lambda\lambda'}$. Since in a disordered system with a magnetic field energy levels are not degenerate, this conclusion is true also when λ stands for energy.

4.3 Dephasing in the ring

The dephasing time is given by the equation [23]:

$$\frac{1}{\tau_{\phi}} = \frac{\tilde{T}}{S\nu\sqrt{D}} \int_0^{\tilde{T}} \frac{d\omega}{\omega^{3/2}}. \quad (\text{A8})$$

The integral in (A8) diverges when $\omega \rightarrow 0$, so that a cut-off has to be introduced. While for the case of a strip the cut-off is $1/\tau_{\phi}$, in case of a ring it must be E_T , due to the argument of [24]. Thus for a ring we have:

$$\frac{1}{\tau_{\phi}} = \frac{\tilde{T}}{S\nu\sqrt{DE_T}} = \frac{\tilde{T}}{g}, \quad g = \frac{\nu DS}{L}.$$

In the diffusion regime $L_{\phi} = \sqrt{D\tau_{\phi}}$, so that

$$\frac{L}{L_{\phi}} = \frac{1}{\sqrt{E_T\tau_{\phi}}} = \sqrt{\frac{\tilde{T}}{gE_T}}.$$

4.4 Average of a Green's function

We calculate $\langle G \rangle$, and then also $\langle GG \rangle$ using the $T = 0$ diagram technique. We can use the $T = 0$ technique for this calculation because the field of impurities is static and thus cannot provide temperature dependence.

After averaging one realizes that series for $\langle G^{(0)}(\vec{p}) \rangle \equiv G(\vec{p})$ implies the following self energy (self-consistent Born approximation, see ([5]39.7):

$$\begin{aligned} \Sigma \equiv \text{[diagram: semi-circle with hatched interior]} &= \text{[diagram: semi-circle with dashed vertical line]}_{q_1} + \text{[diagram: semi-circle with two dashed vertical lines]}_{q_1, q_2} + \text{[diagram: semi-circle with three dashed vertical lines]}_{q_1, q_2, q_3} + \dots \\ &= \frac{1}{2\pi\nu_0\tilde{\tau}V} \sum_{p_1} |G(\vec{p}_1)| + \\ &\quad \frac{1}{(2\pi\nu_0\tilde{q}\tau V)^2} \sum_{p_1, p_2} |U(\vec{p} - \vec{p}_1)|^2 |U(\vec{p} - \vec{p}_1 - \vec{p}_2)|^2 G^2(\vec{p}_1) G(\vec{p}_2) + \dots \end{aligned} \quad (\text{A9})$$

where G stands for G_R , G_A , or time-ordered Green function. For arbitrary realistic impurity potential $U(\vec{p})$ every term in (A9) is finite.

If we define $\Im\Sigma_E \stackrel{\text{df}}{=} -\frac{1}{2\tau_E}$, the average of a Green function will have the form:

$$G(p) = \frac{1}{E - \xi_{\vec{p}} + \frac{i}{2\tau_E} \frac{E}{|\vec{E}|}}, \quad G_{\text{R/A}}(p) = \frac{1}{E - \xi_{\vec{p}} \pm \frac{i}{2\tau_E}}, \quad \tau_E \in \Re. \quad (\text{A10})$$

In (A10) $\xi_{\vec{p}} = \epsilon(\vec{p}) - \mu =$ energy of the particle reckoned from the chemical potential. Let us derive τ_E .

$$\Sigma_{\text{R/A}}(\vec{q}_{\vec{m}}, E) \equiv \Sigma_E(\vec{q}_{\vec{m}}) = \frac{1}{2\pi\nu_0\tilde{\tau}V} \sum_{\vec{n}} \frac{1}{E - \epsilon(\vec{p}_{\vec{n}}) - \Sigma_E(\vec{p}_{\vec{n}})}, \quad (\text{A11})$$

In the approximation with the constant density of states¹³ $\nu(\xi) \approx \nu_0$, (A11) is equivalent to considering only the first term¹⁴ in (A9):

$$\text{Im}\Sigma_{\text{R}}^{(0)} = \frac{1}{2\pi\nu\tau V} \int_{-\infty}^{\infty} d\xi \nu_0 \times \text{Im} \frac{1}{E - \xi + i\delta}, \quad \delta = +0, \quad (\text{A13})$$

$$\text{From (A13) it follows : } \tau_E = \tau_0 = \tilde{\tau}. \quad (\text{A14})$$

In (A13) E -independent part of $\text{Re}\Sigma_E$ is insignificant because it can be absorbed by $\epsilon(\vec{p})$. The E -dependent part can be estimated as $\frac{E}{\tau E_F} \ll E$. Thus one can think that $\text{Re}\Sigma_E = 0$. The situation is different for $\text{Im}\Sigma_E$.

The imaginary part of (A11) gives us an important sum rule for $\text{Im}\Sigma_E \equiv -\frac{1}{2\tau_E}$:

$$\forall E \quad 2\pi\nu_0\tilde{\tau} = \int_{-\infty}^{\infty} d\xi \frac{\nu(\xi)}{(E - \xi)^2 + \frac{1}{4\tau_E^2}} = \frac{1}{V} \sum_{\vec{n} \in \mathbb{Z}^d} G_{\text{R}}(\vec{p}_{\vec{n}}, E) G_{\text{A}}(\vec{p}_{\vec{n}}, E), \quad (\text{A15})$$

From (A15) we see that out of the constant density of states approximation

$$\frac{\tilde{\tau}}{\tau_0} = \frac{\tilde{\nu}}{\nu_0}, \quad \tilde{\nu} \stackrel{\text{df}}{=} \int_{-\infty}^{\infty} \frac{dz}{\pi} \frac{\nu(z/(2\tau_0))}{1 + z^2}. \quad (\text{A16})$$

From Lehmann representation

$$G_{\text{R/A}}(\vec{r}, \vec{r}'; E) = \sum_n \frac{\psi_n(\vec{r})\psi_n^*(\vec{r}')}{E - E_n \pm i\epsilon}, \quad \epsilon = +0 \quad (\text{A17})$$

we see that in case of no interaction between the electrons we have

$$G_{\text{R}}(\vec{r}, \vec{r}'; E) - G_{\text{A}}(\vec{r}, \vec{r}'; E) = -2\pi i \sum_n \delta(E - E_n) \psi_n(\vec{r})\psi_n^*(\vec{r}') \quad (\text{A18})$$

so that

$$\frac{1}{V} \int d^d r [G_{\text{R}}(\vec{r}, \vec{r}; E) - G_{\text{A}}(\vec{r}, \vec{r}; E)] = -2\pi i \nu(E), \quad (\text{A19})$$

where $\nu(E)$ is the density of states defined by (A12). For averaged Green functions (or for a homogeneous system) coordinate integration in (A19) is fictious, because integrand does not depend on coordinates.

From (A19) one obtains:

$$\frac{1}{V} \sum_p [G_{\text{R}}(\vec{p}, E) - G_{\text{A}}(\vec{p}, E)] = -2\pi i \nu(E).$$

Supposing that disorder averaged Green function has the form (A10), we have

$$\forall E \quad \frac{1}{V} \sum_{\vec{p}} \frac{1}{(E - \epsilon(\vec{p}))^2 + \frac{1}{4\tau^2(E)}} = 2\pi\nu_E\tau_E. \quad (\text{A20})$$

Given (A10), from (A20) we have

$$\frac{1}{V} \sum_{\vec{n} \in \mathbb{Z}^d} G_{\text{R}}(\vec{p}_{\vec{n}}, E) G_{\text{A}}(\vec{p}_{\vec{n}}, E) = 2\pi\nu_E\tau_E, \quad (\text{A21})$$

¹³It's definition: (Ω_0 is the complete solid angle; in 3D $\Omega_0 = 4\pi$, in 2D $\Omega_0 = 2\pi$).

$$\nu(\xi) \equiv \frac{1}{V} \sum_{\vec{n}} \delta(\xi + \mu - \epsilon(\vec{p}_{\vec{n}})) \quad \text{so that} \quad \frac{1}{V} \sum_{\vec{p}} = \nu(\xi) d\xi \frac{d\Omega}{\Omega_0}, \quad (\text{A12})$$

¹⁴It is easy to see that due to the analytical properties the other ones = 0. Due to the same reason one can substitute $G \rightarrow G^{(0)}$ in (A9).

so that from (A15) one concludes that

$$\forall E \quad \nu_E \tau_E = \nu_0 \tau_0; \quad \tau_0 = \tilde{\tau}, \quad \tilde{\nu} = \nu_0 = \int_{-\infty}^{\infty} \frac{dz}{\pi} \frac{\nu(z/(2\tau_0))}{1+z^2}, \quad (\text{A22})$$

so that the even part of $\delta\nu_E = \nu_E - \nu_0$ changes its sign, if not $\delta\nu_E \equiv 0$. Eq. (A22) holds for the non-interacting system so that there is no surprise that it is not correct e.g., for the zero bias anomaly.

Let us parametrize¹⁵ dependencies of ν_E and τ_E in the vicinity of point $E = 0$:

$$\begin{aligned} \nu_E &\approx \nu_0 (1 + xE) = \nu_0 + \delta\nu_E, \quad \tau_E \approx \tau_0 (1 - xE), \\ |E| &\lesssim T^*/2, \quad xT^*/2 \ll 1. \end{aligned} \quad (\text{A23})$$

We assume that energy-dependent deviation in (A23) is small for ν : $\delta\nu_E \ll \nu_0$ and for all other quantities: τ_E , D_E (see (A68)), etc. Because integrals $\int d\xi$ converge on $\xi \sim \frac{1}{\tau}$, we also have to impose $x \ll \tau$.

Now let us make some notes about the derivation of (A68). For small q we use an approximation $\epsilon(\vec{p} + \vec{q}) = \epsilon(\vec{p}) + \vec{v}\vec{q} + bq^2/2$. Before performing the integration over ξ one should develop the integrated expression by E , ω and \vec{q} . Then for the zero-order term (A15) is applied; in the other terms one can use (A23) for $\nu(\xi)$. To make $\sum_{\vec{n}} G_R(\vec{p}_{\vec{n}}, E) G_A(\vec{p}_{\vec{n}} - \vec{q}_{\vec{m}}, E - \omega)$ invariant under arbitrary shift in \vec{n} , and in particular, to maintain the obvious relation $\sum_{\vec{n}} G_R(\vec{p}_{\vec{n}}, E) G_A(\vec{p}_{\vec{n}} - \vec{q}_{\vec{m}}, E - \omega) = \sum_{\vec{n}} G_R(\vec{p}_{\vec{n}} + \vec{q}_{\vec{m}}, E) G_A(\vec{p}_{\vec{n}}, E - \omega)$, one has to assume $b = xD_0/\tau_0 = v^2x/d$, so that

$$\epsilon(\vec{p} + \vec{q}) = \epsilon(\vec{p}) + \vec{v}\vec{q} + x \frac{D_0}{2\tau_0} q^2 = \epsilon(\vec{p}) + \vec{v}\vec{q} + x \frac{v^2}{2d} q^2. \quad (\text{A24})$$

From (A24) it follows that usually, when we are not interested in the effects due to the $\nu(\xi) \neq \text{const} = \nu_0$, we can drop quadratic term in the decomposition of $\epsilon(\vec{p} + \vec{q})$.

4.5 Average of two Green's functions: cooperon and diffuson

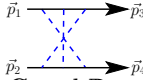
The average of two Green's functions is represented by two sequences of diagrams: the Cooper-alike ladder (named cooperon) and series of maximally anticrossed diagrams (called diffuson):

$$\langle G_R(\vec{p}_1, \vec{p}_3; E) G_A(\vec{p}_2, \vec{p}_4; E') \rangle = \begin{array}{c} \longrightarrow \\ \longrightarrow \end{array} - \begin{array}{c} \longrightarrow \\ \text{---} \\ \longrightarrow \end{array} + \mathbb{C}_{\vec{p}_2, \vec{p}_4; E'}^{\vec{p}_1, \vec{p}_3; E} + \mathbb{D}_{\vec{p}_2, \vec{p}_4; E'}^{\vec{p}_1, \vec{p}_3; E}, \quad (\text{A25})$$

where dashed line stands for impurity averaging [5], and

$$\begin{aligned} \mathbb{C}_{\vec{p}_2, \vec{p}_4; E'}^{\vec{p}_1, \vec{p}_3; E} &= \begin{array}{c} \longrightarrow \\ \text{---} \\ \longrightarrow \end{array} + \begin{array}{c} \longrightarrow \\ \text{---} \\ \longrightarrow \end{array} + \begin{array}{c} \longrightarrow \\ \text{---} \\ \longrightarrow \end{array} + \dots, \\ \mathbb{D}_{\vec{p}_2, \vec{p}_4; E'}^{\vec{p}_1, \vec{p}_3; E} &= \begin{array}{c} \longrightarrow \\ \text{---} \\ \longrightarrow \end{array} + \begin{array}{c} \longrightarrow \\ \text{---} \\ \longrightarrow \end{array} + \begin{array}{c} \longrightarrow \\ \text{---} \\ \longrightarrow \end{array} + \dots \end{aligned} \quad (\text{A26})$$

In the diagrams drawn above, we imply that upper Green function line has energy E , the lower one $-E'$, and momentum variables are placed like in the example:



Here are the expressions for \mathbb{C} and \mathbb{D} :

$$\begin{aligned} \mathbb{C}_{\vec{p}_2, \vec{p}_4; E'}^{\vec{p}_1, \vec{p}_3; E} &= (2\pi)^d \delta(\vec{p}_1 + \vec{p}_2 - (\vec{p}_3 + \vec{p}_4)) G_R(\vec{p}_1, E) G_A(\vec{p}_2, E') \times \\ &\quad \frac{1}{2\pi\nu_0\tilde{\tau}} \cdot \frac{G_R(\vec{p}_3, E) G_A(\vec{p}_4, E')}{1 - X^{(+)}} , \\ \mathbb{D}_{\vec{p}_2, \vec{p}_4; E'}^{\vec{p}_1, \vec{p}_3; E} &= (2\pi)^d \delta(\vec{p}_1 + \vec{p}_4 - (\vec{p}_3 + \vec{p}_2)) G_R(\vec{p}_1, E) G_A(\vec{p}_2, E') \times \\ &\quad \frac{1}{2\pi\nu_0\tilde{\tau}} \cdot \frac{G_R(\vec{p}_3, E) G_A(\vec{p}_4, E')}{1 - X^{(-)}} , \end{aligned} \quad (\text{A27})$$

where

$$\begin{aligned} X^{(+)} &= \frac{1}{2\pi\nu_0\tilde{\tau}} \frac{1}{V} \sum_p G_R(\vec{p}, E) G_A(\vec{p} - (\vec{p}_1 + \vec{p}_2 - 2e\vec{A}), E'), \\ X^{(-)} &= \frac{1}{2\pi\nu_0\tilde{\tau}} \frac{1}{V} \sum_p G_R(\vec{p}, E) G_A(\vec{p} - (\vec{p}_1 - \vec{p}_2), E'). \end{aligned} \quad (\text{A28})$$

More than $\mathbb{C}_{\vec{p}_2, \vec{p}_4; E'}^{\vec{p}_1, \vec{p}_3; E}$ and $\mathbb{D}_{\vec{p}_2, \vec{p}_4; E'}^{\vec{p}_1, \vec{p}_3; E}$, we deal with $C_{\vec{p}_2, \vec{p}_4; E'}^{\vec{p}_1, \vec{p}_3; E}$ and $D_{\vec{p}_2, E'}^{\vec{p}_1, E}$, defined by the following:

$$\begin{aligned} C_{\vec{p}_2, \vec{p}_4; E'}^{\vec{p}_1, \vec{p}_3; E} &= (2\pi)^d \delta(\vec{p}_1 + \vec{p}_2 - (\vec{p}_3 + \vec{p}_4)) G_R(\vec{p}_1, E) G_A(\vec{p}_2, E') G_R(\vec{p}_3, E) G_A(\vec{p}_4, E') C_{\vec{p}_2, E'}^{\vec{p}_1, E}, \\ D_{\vec{p}_2, \vec{p}_4; E'}^{\vec{p}_1, \vec{p}_3; E} &= (2\pi)^d \delta(\vec{p}_1 + \vec{p}_4 - (\vec{p}_3 + \vec{p}_2)) G_R(\vec{p}_1, E) G_A(\vec{p}_2, E') G_R(\vec{p}_3, E) G_A(\vec{p}_4, E') D_{\vec{p}_2, E'}^{\vec{p}_1, E}. \end{aligned} \quad (\text{A29})$$

¹⁵An example where one need to introduce see (A23) - like dependence is the thermoelectric effect, see- [25], p. 103.

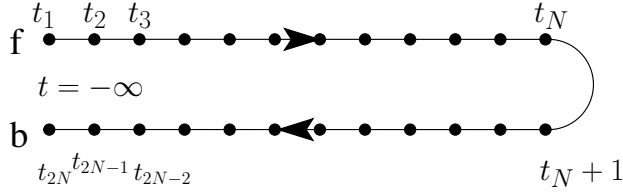


Figure 18: The Keldysh contour.

$$C_{\vec{k}-\vec{p}, E-\omega}^{\vec{p}, E} = \frac{1}{2\pi\nu_0\tau_0\tau_\epsilon - i\omega + D_\epsilon k^2}; \quad (\text{A30})$$

$$D_{\vec{p}-\vec{k}, E-\omega}^{\vec{p}, E} = \frac{1}{2\pi\nu_0\tau_0\tau_\epsilon - i\omega + D_\epsilon k^2}; \quad (\text{A31})$$

Notice that (A30) and (A31) differ from their values for $\nu(\xi) = \text{const}$ only by substitution of τ , D with their energy dependent generalizations τ_ϵ , D_ϵ , etc.

Now let us consider the case of constant density of states. There is no energy transfer in cooperon or diffuson lines, so in energy representation we have simple products of the type: $G_R(E_1)G_R(E_1)\Sigma_{E_2}^{E_1}G_A(E_2)G_A(E_2)$. In time representation we get convolution. Let us write out the expressions for $\Sigma(C)$ and $\Sigma(D)$ in momentum- time representation (with the removed $(2\pi)^2\delta(E_1 - E_3)\delta(E_2 - E_4)$):

$$C(\vec{p}_1, \vec{p}_2; t) = \frac{(2\pi)^d \delta(\vec{p}_1 + \vec{p}_2 - (\vec{p}_3 + \vec{p}_4)) \delta(t + t_2) \theta(t) \exp \left[-Dt \left(\vec{p}_1 + \vec{p}_2 - 2e\vec{A} \right)^2 \right]}{2\pi\nu_0\tau^2}; \quad (\text{A32})$$

$$D(\vec{p}_1, \vec{p}_2; t) = \frac{(2\pi)^d \delta(\vec{p}_1 + \vec{p}_4 - (\vec{p}_3 + \vec{p}_2)) \delta(t + t_2) \theta(t) \exp \left[-Dt \left(\vec{p}_1 - \vec{p}_2 \right)^2 \right]}{2\pi\nu_0\tau^2}; \quad (\text{A33})$$

4.6 Keldysh technique

STOP **Note 01.04.2009:** Better see sections ?? and ?? from my notes [7]. Consider the case of a quasiequilibrium state [21] when an external fixed parameter is the energy distribution function, see sec. 4.2. The Keldysh technique is derived exactly in the same manner as the $T = 0$ one; the difference stands in the substitution of the time ordering by the Keldysh contour ordering T_{C_K} , see fig. 18.

$$G_{C_K}(x, x') \equiv -i \langle T_c [\psi(x) \psi^\dagger(x')] \rangle. \quad (\text{A34})$$

Then we can map G_{C_K} onto 2×2 matrix, so that the first argument of the Green function corresponds to the upper part of the contour, while the second argument - to the lower part. One immediately notes that we are almost always interested in the off-diagonal elements of this matrix, which gives the density matrix - like quantities (A38). Then using (A80) we transform our 2×2 matrix

$$\begin{aligned} G_{C_K} &\leftrightarrow \begin{pmatrix} G_{ff} & G_{fb} \\ G_{bf} & G_{bb} \end{pmatrix} = \begin{pmatrix} -i \langle T[\psi(x) \psi^\dagger(x')] \rangle & -i \eta \langle \psi^\dagger(x') \psi(x) \rangle \\ -i \langle \psi(x) \psi^\dagger(x') \rangle & -i \langle \tilde{T}[\psi(x) \psi^\dagger(x')] \rangle \end{pmatrix} = \\ &= \frac{1}{2} \begin{pmatrix} G_R^{(+)} + G_R^{(-)} - \eta \left(G_A^{(+)} - G_A^{(-)} \right) & \eta \left[G_R^{(+)} - G_R^{(-)} - \left(G_A^{(+)} - G_A^{(-)} \right) \right] \\ G_R^{(+)} + G_R^{(-)} - \left(G_A^{(+)} + G_A^{(-)} \right) & - \left(G_A^{(+)} + G_A^{(-)} \right) + \eta \left(G_R^{(+)} - G_R^{(-)} \right) \end{pmatrix} = \\ &= \frac{1}{2} \begin{pmatrix} G_K + (G_R + G_A) & G_K - (G_R - G_A) \\ G_K + (G_R - G_A) & G_K - (G_R + G_A) \end{pmatrix} \equiv \Gamma, \end{aligned} \quad (\text{A35})$$

where T and \tilde{T} stand for normal and inverse time ordering; all Green functions have (x, x') arguments. It is more convinient to work in the representation where Green function is given by the upper triangular matrix

$$G = \begin{pmatrix} G_R & G_K \\ 0 & G_A \end{pmatrix} = L \sigma_3 \Gamma L^{-1}, \quad L = \frac{\sigma_0 - i\sigma_2}{\sqrt{2}}, \quad (\text{A36})$$

where σ_i stand for Pauli matrices. The transformation (A36) is also responsible for the form of emission and absorption matrices (33).

With the notations (A79) we have from ([14]2.22) (in the following, upper signs stand for bosons and the lower ones - for fermions):

$$G_K(\lambda, \lambda') = -i \langle [\psi(\lambda), \psi^\dagger(\lambda')]_{\pm} \rangle = G_R^{(\pm)}(\lambda, \lambda') - G_A^{(\pm)}(\lambda, \lambda'), \quad (\text{A37})$$

Note that $G_{\text{R/A}}^{(\mp)}$ are the usual retarded and advanced Green functions (see [5]).

One obtains that for fermions

$$\begin{aligned}\langle \psi(\lambda)\psi^\dagger(\lambda') \rangle &= \frac{i}{2} [G_{\text{R}}(\lambda, \lambda') - G_{\text{A}}(\lambda, \lambda') + G_{\text{K}}(\lambda, \lambda')], \\ \langle \psi^\dagger(\lambda')\psi(\lambda) \rangle &= \frac{i}{2} [G_{\text{R}}(\lambda, \lambda') - G_{\text{A}}(\lambda, \lambda') - G_{\text{K}}(\lambda, \lambda')].\end{aligned}\quad (\text{A38})$$

The expression for the operator of current density (in the interaction representation):

$$\hat{j}(x) = \frac{ie\hbar}{2m} [(\nabla\psi^\dagger(x))\psi(x) - \psi^\dagger(x)(\nabla\psi(x))] - \frac{e^2}{mc}\vec{A}(x)\psi^\dagger(x)\psi(x); \quad x \equiv (\vec{r}, t) \quad (\text{A39})$$

From (A39) we obtain the formula for the current of fermions (keeping in mind (A2)):

$$\begin{aligned}\vec{j}(\vec{r}) &= \frac{e\hbar}{4m} \int_{-\infty}^{\infty} \frac{dE}{2\pi} \lim_{\vec{r}' \rightarrow \vec{r}} \left(\vec{\nabla}_{\vec{r}} - \vec{\nabla}_{\vec{r}'} - 2i \frac{e}{\hbar c} \vec{A} \right) [G_{\text{R}} - G_{\text{A}} - G_{\text{K}}](\vec{r}, \vec{r}'; E) = \\ &= -\frac{e\hbar}{4m} \int_{-\infty}^{\infty} \frac{dE}{2\pi} \lim_{\vec{r}' \rightarrow \vec{r}} \left(\vec{\nabla}_{\vec{r}} - \vec{\nabla}_{\vec{r}'} - 2i \frac{e}{\hbar c} \vec{A} \right) G_{\text{K}}(\vec{r}, \vec{r}'; E) = \\ &= \int \frac{dE}{2\pi} \frac{1}{V} \sum_{\vec{p}} \frac{1}{2} \hat{j}(\vec{p}) G_{\text{K}}(\vec{p}, E),\end{aligned}\quad (\text{A40})$$

where $\hat{j}(\vec{p})$ is defined in (37).

From ([22]2.8) and ([22]2.10) it follows that in equilibrium $G^{(+)} = G^{(-)} \coth \frac{\beta E}{2}$, and we obtain that

$$G_{\text{K}} = h(G_{\text{R}} - G_{\text{A}}) \quad (\text{A41})$$

with h from (A45). In equilibrium from (A40) and (A41) one obtains (2). In our article [26] (see sec. 3.3) we argue (though do not prove rigorously) that $G_{\text{R/A}}$ contain the information only about diagonal matrix elements¹⁶. Thus any physical quantity defined using $G_{\text{R/A}}$ (like tunnel density of states) can be written in an equilibrium form (see (2) as an example):

$$O = \int dE \frac{1}{1 + e^{E/T}} O(E). \quad (\text{A42})$$

Let us consider an equilibrium of non-interacting particles in some external potential, so that λ is a conserving quantity. From (A82) and (A83) we get:

$$G_{\text{R}}^{(\pm)(0)}(\lambda, E) = \frac{h_{\text{B/F}}(\xi_\lambda)}{E - \xi_\lambda + i\delta}, \quad G_{\text{A}}^{(\pm)(0)}(\lambda, E) = \frac{h_{\text{B/F}}(\xi_\lambda)}{E - \xi_\lambda - i\delta}, \quad \delta = +0, \quad (\text{A43})$$

$$G_{\text{K}}^{(0)}(\lambda, E) = h_{\text{B/F}}(\xi_\lambda) \left(G_{\text{R}}^{(\mp)(0)}(\lambda, E) - G_{\text{A}}^{(\mp)(0)}(\lambda, E) \right), \quad (\text{A44})$$

$$h_{\text{B}}(E) = \coth \frac{1}{2}\beta E, \quad h_{\text{F}}(E) = \tanh \frac{1}{2}\beta E. \quad (\text{A45})$$

In the bosonic case ξ_λ is the energy of a boson; In the fermionic case ξ_λ is the energy of a fermion reckoned from the Fermi energy.

We have from (A44):

$$G_{\text{K}}^{(0)}(\lambda, E) = -2\pi i \times h_{\text{B/F}}(\xi_\lambda) \times \delta(E - \xi_\lambda),$$

so that (in accordance with eqs. (3.21) and (2.66) from [14], and (A41))

$$G_{\text{K}}^{(0)}(\lambda, E) = h_{\text{B/F}}(E) \left(G_{\text{R}}^{(\mp)(0)}(\lambda, E) - G_{\text{A}}^{(\mp)(0)}(\lambda, E) \right). \quad (\text{A46})$$

Let us now concentrate on the case of electrons. We are used to work with their Green functions averaged over the interaction with randomly placed impurities. After the averaging we get

$$\langle G_{\text{K}}(\vec{p}, E) \rangle = h_{\text{F}}(E) (\langle G_{\text{R}}(\vec{p}, E) \rangle - \langle G_{\text{A}}(\vec{p}, E) \rangle), \quad (\text{A47})$$

where $G_{\text{R/A}}$ are given by (A10).

4.7 Screening

In this section all the calculations are done for the case of small value of excitation momentum q . To consider the case of large q one should know the dependence of energy on momentum (which we actually never know). However, one can suppose $E(p) = \frac{p^2}{2m}$ and do this (quite long) calculation. It must be just this is the way it is done in [27], pp. 158-163.

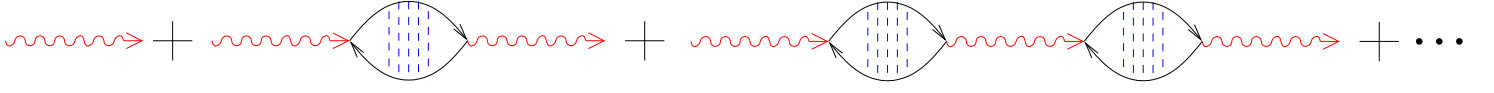


Figure 19: Screening in RPA approximation (wavy lines stand for bare interaction, dashed ones - for the impurity averaging lines composing diffuson). The possibility of connecting of bubbles with “external” green function lines should not be considered here, for it is taken into account when considering diagrams with higher order on interaction. Studying these higher order diagrams, one can detect some other (like RPA or the renormalization in Cooper channel) essential infinite sequence of diagrams. The same is true for the lines connecting different bubbles.

Because of the long-range character of Coulomb interaction, it must not be considered in the first several orders of the perturbation theory. Instead, screening must be taken into account, which is technically done by summation of infinite number of diagrams.

The renormalized interaction matrix is defined by

$$\tilde{U}(q) = \frac{U(q)}{1 - \text{bubble}} = \frac{U(q)}{1 - \Pi(q)U(q)}. \quad (\text{A48})$$

The first and the second diagrams (their matrix kk' components) in Fig. 19 are respectively equal to $V\delta_{\vec{q},\vec{q}'}U(q)\tau_{kk'}^0$ and

$$-iU(q)U(q')\text{Sp} \left[\frac{1}{V^2} \sum_{p,p'} \int \frac{dE}{2\pi} \gamma^k \hat{G}(\vec{p}, \vec{p}'; E) \tilde{\gamma}^{k'} \hat{G}(\vec{p}' - \vec{q}', \vec{p} - \vec{q}; E - \omega) \right],$$

where matrices γ and $\tilde{\gamma}$ are given by eq. (33).

The polarization thus is given by

$$V\delta_{\vec{q},\vec{q}'}\Pi(q) = -i\langle \text{Sp} \left[\frac{1}{V^2} \sum_{p,p'} \int \frac{dE}{2\pi} \gamma^k \hat{G}(\vec{p}, \vec{p}'; E) \tilde{\gamma}^{k'} \hat{G}(\vec{p}' - \vec{q}', \vec{p} - \vec{q}; E - \omega) \right] \rangle. \quad (\text{A49})$$

From (A49), (A41) and (A29) it follows that

$$V\delta_{\vec{q},\vec{q}'}\Pi_R(q) = -\frac{i}{2} \frac{1}{V^2} \sum_{p,p'} \int \frac{dE}{2\pi} \left\{ D_{\vec{p}-\vec{q},\vec{p}';E-\omega}^{\vec{p},\vec{p}';E} (h_E - h_{E-\omega}) + V^2 \delta_{\vec{p},\vec{p}'} \delta_{\vec{q},\vec{q}'} [G_R(p)G_R(p-q)h_{E-\omega} - G_A(p)G_A(p-q)h_E] \right\}, \quad (\text{A50})$$

$$V\delta_{\vec{q},\vec{q}'}\Pi_A(q) = -\frac{i}{2} \frac{1}{V^2} \sum_{p,p'} \int \frac{dE}{2\pi} \left\{ -D_{\vec{p}',\vec{p};E}^{\vec{p}',\vec{p}';E-\omega} (h_E - h_{E-\omega}) + V^2 \delta_{\vec{p},\vec{p}'} \delta_{\vec{q},\vec{q}'} [G_R(p)G_R(p-q)h_E - G_A(p)G_A(p-q)h_{E-\omega}] \right\}, \quad (\text{A51})$$

$$V\delta_{\vec{q},\vec{q}'}\Pi_K(q) = -\frac{i}{2} \frac{1}{V^2} \sum_{p,p'} \int \frac{dE}{2\pi} \left\{ \left[D_{\vec{p}-\vec{q},\vec{p}';E-\omega}^{\vec{p},\vec{p}';E} + D_{\vec{p}',\vec{p};E}^{\vec{p}',\vec{p}';E-\omega} \right] (1 - h_E h_{E-\omega}) + V^2 \delta_{\vec{p},\vec{p}'} \delta_{\vec{q},\vec{q}'} [G_R(p)G_R(p-q) + G_A(p)G_A(p-q)] h_E h_{E-\omega} \right\}. \quad (\text{A52})$$

In (A50-A52) D denotes diffuson \mathbb{D} together with the zeroth-order term \longrightarrow privated of impurity lines, see (A25), (A26), and (A27).

From the conservation of total number of particles one realizes that

$$\text{for } \vec{q} = 0 \text{ and } \forall \omega \quad \Pi_{R/A}(\vec{q}, \omega) = 0. \quad (\text{A53})$$

From (A50), (A51) and (A52) we realize that if one ignores effects due to the energy dependence of the density of states or in the equilibrium (A41) holds **exactly** for the polarization and hence for the renormalized potential. In the equilibrium case using (A85) one recovers (A45).

¹⁶One can think about an analogy: in the 2×2 matrix Green function they stand on diagonal, so they know only about diagonal elements of the density matrix.

One can see that

$$\text{Supp} [1 - h_{E+\omega/2} h_{E-\omega/2}] = \text{Supp} [h_{E+\omega/2} - h_{E-\omega/2}] = \left\{ E : |E| \lesssim \max \left(\frac{\tilde{T}}{2}, \frac{\omega}{2} \right) \right\},$$

so that in (A52) energy integration is limited in the zone where we can use (A23). It also means that in (A50), (A51) and (A52), we are free to

- when considering non-pole contributions: to substitute $h_E \leftrightarrow h_{E-\omega}$ and $h_E h_{E-\omega} \leftrightarrow 1$.
- when considering pole contributions having $(h_E - h_{E-\omega})$ and $(1 - h_E h_{E-\omega})$ multipliers: to substitute $\frac{1}{V} \sum_{\vec{p}_n} \rightarrow \int d\xi \nu(\xi)$ with weak $\nu(\xi)$ dependence (A23) and to integrate over ξ before integrating over energy.

So we see that (due to $\int \frac{dE}{2\pi}$) non-pole terms give zero contribution to (A52).

Let us introduce a quantity

$$\tilde{\nu}(q) = \frac{i}{2} \frac{1}{V} \sum_{\vec{p}_n} \int \frac{dE}{2\pi} h_E [G_R(p) G_R(p-q) - G_A(p) G_A(p-q)] \in \Re.$$

$$\text{If } \nu \text{ is a constant, then } \tilde{\nu}(q) = \tilde{\nu}(0) = \nu_0 \int dE h'_E / 2 = \nu_0.$$

$$\begin{aligned} \frac{1}{V^2} \sum_{p,p'} D_{\vec{p}-\vec{q}, \vec{p}'-\vec{q}'; E-\omega}^{\vec{p}, \vec{p}'; E} &= 2\pi \nu_0 \tilde{\tau} \left(\frac{1}{1-X(q)} - 1 \right) V \delta_{\vec{q}, \vec{q}'}, \\ \frac{1}{V^2} \sum_{p,p'} D_{\vec{p}', \vec{p}; E}^{\vec{p}'-\vec{q}', \vec{p}-\vec{q}; E-\omega} &= 2\pi \nu_0 \tilde{\tau} \left(\frac{1}{1-X^*(q)} - 1 \right) V \delta_{\vec{q}, \vec{q}'}, \end{aligned} \quad (\text{A54})$$

where $X(q)$ is given by (A65).

$$\begin{aligned} \Pi_R(q) &= \Pi_A^*(q) = -\frac{i\nu_0 \tilde{\tau}}{2} \int dE \frac{X(q)(h_E - h_{E-\omega})}{1-X(q)} - \tilde{\nu}(q), \\ \Pi_K(q) &= -\frac{i\nu_0 \tilde{\tau}}{2} \int dE \left[\frac{X(q)}{1-X(q)} + \frac{X^*(q)}{1-X^*(q)} \right] (1 - h_E h_{E-\omega}) \in \Im. \end{aligned} \quad (\text{A55})$$

Note that in general case Π_K is not proportional to $\Pi_R - \Pi_A$, so that (A41) does not hold.

The simplest form the interaction has for large values of momentum $\sim p_F$. From (A67) we deduce that in this case

$$U_K = 0, \quad U_R = U_A = \frac{1}{\tilde{\nu}} \equiv \frac{\Lambda}{\nu_0}, \quad \tilde{\nu} \stackrel{\text{df}}{=} \lim_{q \rightarrow \infty} \tilde{\nu}(q), \quad \Lambda \stackrel{\text{df}}{=} \frac{\nu_0}{\tilde{\nu}}. \quad (\text{A56})$$

When one does not take into account the ν_E - dependence, the polarization simplifies substantially:

$$\begin{aligned} \Pi_R(q) &= \Pi_A^*(q) = -\nu_0 \left[1 + i\omega \tilde{\tau} \frac{X(q)}{1-X(q)} \right], \\ \Pi_K(q) &= -2i\nu_0 \tilde{\tau} \tilde{T}_\omega \left[\frac{X(q)}{1-X(q)} + \frac{X^*(q)}{1-X^*(q)} \right], \end{aligned} \quad (\text{A57})$$

where

$$\tilde{T} \equiv \tilde{T}_0; \quad \tilde{T}_\omega = \tilde{T}_{-\omega} \equiv \tilde{T}(\omega) = \frac{1}{4} \int_{-\infty}^{\infty} dE (1 - h_E h_{E-\omega}) = \boxed{\text{in equilibrium}} = \frac{\omega}{2} \coth \frac{\omega}{2T} \xrightarrow{\omega \rightarrow 0} T.$$

From (A57) for arbitrary $X(q)$ we arrive to

$$\forall \omega \in \mathbb{C} \quad \tilde{U}_K = \frac{2\tilde{T}_\omega}{\omega} (\tilde{U}_R - \tilde{U}_A); \quad \forall \omega \in \Re \quad \tilde{U}_R(q) = \tilde{U}_A^*(q).$$

In 2D $u^{-1}(q) \propto \nu_0 q r_B$; in 3D $u^{-1}(q) \propto \nu_0 (q r_B)^2$. Usually $q \sim 1/L$ so that in Dyson equation (A48) one can neglect $u^{-1}(q)$. As a result, $U_{R/A/K}$ do not depend on original, unscreened Coulomb potential (such situation is called *universal limit*).

In the diffusion approximation

$$\Pi_{R/A}(q) = -\frac{\nu_0 D q^2}{D q^2 \mp i\omega}, \quad \Pi_K(q) = -\frac{4\nu_0 i D q^2 \tilde{T}_\omega}{D^2 q^4 + \omega^2}. \quad (\text{A58})$$

In 2D case, where $U(q) = 2\pi e^2/q$ we have

$$\begin{aligned} \tilde{U}_{R/A}(q) &= \frac{2\pi e^2}{q} - \frac{4\pi^2 e^4 D \nu_0}{D q (q + 2\pi e^2 \nu_0) \mp i\omega} = \frac{1}{\nu_0} \frac{1}{\frac{q}{2\pi \nu_0 e^2} + \frac{D q^2}{D q^2 \mp i\omega}}, \\ \tilde{U}_K(q) &= -\frac{16i\pi^2 e^4 D \nu_0 \tilde{T}_\omega}{D^2 q^2 (q + 2\pi e^2 \nu_0)^2 + \omega^2} = -\frac{4\tilde{T}_\omega}{D q^2} \cdot \frac{i\nu_0}{\left(\frac{q}{2\pi e^2} + \nu_0 \right)^2 + \left(\frac{\omega}{2\pi e^2 D q} \right)^2}. \end{aligned} \quad (\text{A59})$$

In 2D $\frac{1}{2\pi e^2 \nu_0} \sim \frac{\pi}{e^2 \nu_0} = r_B = \text{Bohr radius}$.

Like in [28], we want to neglect $\frac{q}{2\pi e^2}$ in the denominator of (A59). We can do it in case

$$\omega \ll Dq/r_B \ll D/\tau_B^2 \quad (\text{A60})$$

and obtain¹⁷

$$U_{R/A}(q) \approx \frac{1}{\nu_0} \left(1 \mp \frac{i\omega}{Dq^2} \right), \quad \tilde{U}_K(q) \approx \frac{-4i\tilde{T}_\omega}{\nu_0 Dq^2}. \quad (\text{A61})$$

The condition (A60) holds in the *diffusion regime*, when $Dq^2 \sim |\omega| \ll 1/\tau$.

Let us now go out of the diffusion approximation: still $q \ll p_F$ but $ql \gg 1$. Then

$$\Pi_{R/A}(q) = -\nu_0 \left[1 \pm \frac{i\omega\tau}{lq} \right], \quad \Pi_K(q) = -\frac{4i\nu_0\tau}{lq} \tilde{T}_\omega,$$

so that

$$U_{R/A}(q) = \frac{1}{\nu_0 \left(1 \pm \frac{i\omega\tau}{lq} \right)}, \quad \tilde{U}_K(q) = \frac{1}{\nu_0} \frac{4i\tilde{T}_\omega\tau}{lq} \frac{1}{1 + \left(\frac{\omega\tau}{lq} \right)^2}. \quad (\text{A62})$$

From (A65), (44), (A61), (A62) and (A67) one concludes that for $Dq \gg |\omega|$ the potential does not depend on q .

4.8 Other formulas

In this subsection we use the following notations:

$$\forall \vec{a}, \vec{b} \in \mathbb{C}^d \quad \vec{a} \circ \vec{b} \equiv (a_1 b_1, a_2 b_2, \dots, a_d b_d)^T, \quad \vec{a} (\vec{b} \circ \vec{c}) = (\vec{a} \circ \vec{b}) \vec{c}, \\ \vec{a}/\vec{b} \equiv (a_1/b_1, a_2/b_2, \dots, a_d/b_d)^T. \quad (\text{A63})$$

In d dimensions we have:

$$\int \frac{d\Omega}{\Omega_0} n_i n_j = \frac{\delta_{ij}}{d}. \quad (\text{A64})$$

Let us introduce quantity

$$X(q; E, E') \stackrel{\text{df}}{=} \frac{1}{2\pi\nu_0\tilde{\tau}} \frac{1}{V} \sum_{\vec{n}} G_R(\vec{p}_{\vec{n}}, E) G_A(\vec{p}_{\vec{n}} - \vec{q}, E'), \quad X(q) \equiv X(\vec{q}, \omega) = X(q; E, E - \omega) \quad (\text{A65})$$

From (A15) $X(\vec{0}, 0) = 1$. For $q \ll p_F$:

$$\boxed{\text{in 2D}} \quad X(\vec{q}, \omega) = \frac{1}{\sqrt{l^2 q^2 - (i \pm \omega\tau)^2}}, \quad \boxed{\text{in 3D}} \quad X(\vec{q}, \omega) = \frac{1}{2ilq} \log \frac{1 - i\omega\tau + ilq}{1 - i\omega\tau - ilq} \quad (\text{A66})$$

The asymptotic for $q \gtrsim p_F$ depends on the particular dispersion law, but generally $X(\vec{q}, \omega)$ must decrease while q enlarges:

$$\lim_{q \rightarrow \infty} X(\vec{q}, \omega) = 0. \quad (\text{A67})$$

In the diffusion approximation using¹⁸ (A15), (A23) and (A22) we have

$$X(\vec{q}; E, E') = 1 - \tau_\epsilon \tau_0 / \tilde{\tau} \times [D_\epsilon q^2 - i\omega] \approx_{x \rightarrow 0} 1 - \tau (Dq^2 - i\omega), \quad \epsilon = \frac{E+E'}{2}, \\ \nu(\xi) \approx \nu_0(1 + x\xi), \quad \tau_E \equiv \tau(E) \approx \tau_0(1 - xE), \quad l_E = v\tau_E, \quad D_E = \frac{l_E^2}{d\tau_E}. \quad (\text{A68})$$

Note that E -dependent corrections of (A68) make sense if (in case of cooperon/diffuson) we are near enough to the pole. More precisely, a condition $\omega(\omega + 3D_0 q^2)\tau_0 \ll x\epsilon[2D_0 q^2 - i\omega]$ must hold; otherwise we go under the precession of the diffusion approximation. In particular, these corrections *are important* when $Dq^2 \sim \omega \ll x\epsilon/\tau_0$.

The result (A68) is consistent with the general requirement: cooperon's diffusion coefficient is a symmetric function of E and E' ; this becomes clear if one considers cooperon plus its complex conjugate (which should certainly be a real quantity).

¹⁷Note that (A61) is correct in arbitrary dimension.

¹⁸To obtain (A68), we at first expanded $G_A(\vec{p} - \vec{q}, E - \omega)$ by \vec{q}, ω ; then used (A15) for the zeroth-order term, then substituted (A23) and at last integrated by $d\xi \frac{d\Omega}{\Omega_0}$.

The expression for the current of arbitrary particles and its operator with charge e in gauge with scalar potential = 0 (see eqs. (115.4) and (115.6) from [29]):

$$\vec{j}(x) = \frac{ie\hbar}{2m} [(\nabla\psi^*(x))\psi(x) - \psi^*(x)(\nabla\psi(x))] - \frac{e^2}{mc}\vec{A}(x)\psi^*(x)\psi(x) + \frac{\mu c}{s}\mathbf{rot}\left[\psi^*(x)\hat{s}\psi(x)\right], \quad (\text{A69})$$

$$\begin{aligned} \vec{j}_{ab}(x) &= \frac{ie\hbar}{2m} [(\nabla\psi_a^*(x))\psi_b(x) - \psi_a^*(x)(\nabla\psi_b(x))] - \\ &\quad \frac{e^2}{mc}\vec{A}(x)\psi_a^*(x)\psi_b(x) + \frac{\mu c}{s}\mathbf{rot}\left[\psi_a^*(x)\hat{s}\psi_b(x)\right]. \end{aligned} \quad (\text{A70})$$

Due to the application of a constant vector potential Green function changes like (see [30])

$$G(\vec{r}, \vec{A}) = G(\vec{r}, \vec{A} = 0)e^{ie\vec{A}\vec{r}}. \quad (\text{A71})$$

The density of states for systems with no interactions between the electrons:

$$\text{in 1D } \nu_0 = \frac{m}{2\pi p_F}, \text{ in 2D } \nu_0 = \frac{m}{2\pi\hbar}, \text{ in 3D } \nu_0 = \frac{mp_F}{2\pi^2\hbar^2}, \quad (\text{A72})$$

Poisson formula:

$$\sum_{n \in \mathbb{Z}} \delta(x - n) = \sum_{m \in \mathbb{Z}} e^{2\pi i m x} \quad (\text{A73})$$

From (A73) we get:

$$\sum_{n \in \mathbb{Z}} f(n + \xi) = \sum_{m \in \mathbb{Z}} e^{-2\pi i m \xi} \times \int e^{2\pi i m x} f(x) dx. \quad (\text{A74})$$

Using (A74), we arrive to a useful relation:

$$\begin{aligned} \frac{1}{V} \sum_{\vec{n} \in \mathbb{Z}^d} f(\vec{p}_{\vec{n}} - 2e\vec{A}) &= \sum_{\vec{n} \in \mathbb{Z}^d} \exp\left[2\pi i \vec{n} \frac{\vec{\Phi}}{\Phi_0} \frac{e}{|e|}\right] \times \int \frac{d^d p}{(2\pi)^d} e^{i\vec{p}(\vec{n} \circ \vec{L})} f(\vec{p}), \\ \vec{L} &= (L_x, L_y, \dots)^T, \quad \vec{p}_{\vec{n}} = 2\pi \vec{n} / \vec{L}, \quad \vec{\Phi} = \vec{A} \circ \vec{L}, \quad \Phi_0 = \pi / |e|, \end{aligned} \quad (\text{A75})$$

where the circle in $(\vec{n} \circ \vec{L})$ and $\vec{A} \circ \vec{L}$ denotes component multiplication of vectors, see (A63).

$$\begin{aligned} \int_{-\infty}^{\infty} e^{i\vec{p}\vec{z}} (2\vec{p} - \vec{q})_{\alpha\beta} \exp[-p^2 x^2 - y^2(\vec{p} - \vec{q})^2] d^2 p &= \\ \pi \frac{2(x^2 + y^2)\delta_{\alpha\beta} + [\vec{q}(x^2 - y^2) - i\vec{z}]_{\alpha\beta}}{(x^2 + y^2)^3} \exp\left[-\frac{x^2 y^2 q^2 + z^2/4}{x^2 + y^2}\right] \exp\left[\frac{iy^2 \vec{z}\vec{q}}{x^2 + y^2}\right] &= \\ \frac{2\pi}{\tau_1^2} \exp\left[-\frac{(\tau_1 \vec{q} - i\vec{z})^2}{4\tau_1}\right] \exp\left[-\frac{z^2}{2\tau_1}\right] \times \left(\delta_{\alpha\beta} + \frac{1}{2\tau_1} [\tau_2 \vec{q} - i\vec{z}]_{\alpha\beta}\right) \exp\left[\frac{\tau_2^2 q^2 - 2i\tau_2 \vec{z}\vec{q}}{4\tau_1}\right], \end{aligned} \quad (\text{A76})$$

where

$$x^2 + y^2 = \tau_1, \quad x^2 - y^2 = \tau_2, \quad x^2 = \frac{\tau_1 + \tau_2}{2}, \quad y^2 = \frac{\tau_1 - \tau_2}{2}. \quad (\text{A77})$$

$$\begin{aligned} \int \frac{d^d k}{(2\pi)^d} \vec{k} \exp\left[i(\vec{L} \circ \vec{m}) \vec{k} - Dtk^2\right] &= \frac{i\vec{L} \circ \vec{m}}{2Dt} (4\pi Dt)^{-d/2} \exp\left[-\frac{(\vec{L} \circ \vec{m})^2}{4Dt}\right], \\ \int \frac{d^d k}{(2\pi)^d} \exp\left[i(\vec{L} \circ \vec{m}) \vec{k} - Dtk^2\right] &= (4\pi Dt)^{-d/2} \exp\left[-\frac{(\vec{L} \circ \vec{m})^2}{4Dt}\right] \end{aligned} \quad (\text{A78})$$

We use some definitions in Heisenberg representation from [22] (however, changing signs in them order to have correspondence with [5]):

$$\begin{aligned} G_R^{(\pm)}(x, x') &\equiv -K_R^{(\pm)}(x, x') = -i\theta(t - t') \langle [\psi(x), \psi^\dagger(x')]_{\pm} \rangle, \\ G_A^{(\pm)}(x, x') &\equiv -K_A^{(\pm)}(x, x') = i\theta(t' - t) \langle [\psi(x), \psi^\dagger(x')]_{\pm} \rangle, \\ G_{R/A}^{\sim}(x, x') &\equiv -K_{R/A}(x, x') = \mp i\theta[\pm(t - t')] \langle \psi(x)\psi^\dagger(x') \rangle, \\ G(x, x') &\equiv -K_C(x, x') \equiv -i\langle T[\psi(x)\psi^\dagger(x')] \rangle, \end{aligned} \quad (\text{A79})$$

$$G_{\text{R/A}}^{(+)} + G_{\text{R/A}}^{(-)} = 2\tilde{G}_{\text{R/A}}, \quad G_C = \tilde{G}_R - \eta\tilde{G}_A, \quad (\text{A80})$$

where $\eta = \pm 1$ for the case of bosons and fermions respectively.

$$\text{In energy representation} \quad K_{\text{R/A}}(E) = -\frac{1}{2\pi}G_{\text{R/A}}(E). \quad (\text{A81})$$

For fermions, $G_{\text{R/A}} \equiv G_{\text{R/A}}^{(+)}$ (and for bosons $G_{\text{R/A}} \equiv G_{\text{R/A}}^{(-)}$) obey the simplest equations, and this must be the reason why just they are usually considered, see ([22]6.2-4). In equilibrium any Green function can be obtained from any other one using spectral function, see [22].

From [22] we have in case of non-interacting fermions in equilibrium:

$$G_{\text{R/A}}^{(+)(0)}(\lambda) = \frac{1}{E - \epsilon(\lambda) \pm i\delta}, \quad G_{\text{R/A}}^{(0)}(\lambda) = \frac{1 - n_F}{E - \epsilon(\lambda) \pm i\delta}, \quad \delta = +0. \quad (\text{A82})$$

One can easily do also the case of non-interacting bosons in equilibrium:

$$G_{\text{R/A}}^{(-)(0)}(\lambda) = \frac{1}{E - \epsilon(\lambda) \pm i\delta}, \quad G_{\text{R/A}}^{(0)}(\lambda) = \frac{1 + n_B}{E - \epsilon(\lambda) \pm i\delta}, \quad \delta = +0. \quad (\text{A83})$$

In these relations $n_{B/F} = \frac{1}{e^{\epsilon/T} \mp 1}$ are Bose and Fermi distributions. Moreover, for arbitrary h_E (i.e. also for out-of-equilibrium systems):

$$\forall \omega \quad \int_{-\infty}^{+\infty} dE (h_E - h_{E-\omega}) = 2\omega. \quad (\text{A84})$$

A useful identity:









$$\forall E, \omega, T \quad \left(\tanh \frac{E}{2T} - \tanh \frac{E-\omega}{2T} \right) \coth \frac{\omega}{2T} = 1 - \tanh \frac{E}{2T} \tanh \frac{E-\omega}{2T}. \quad (\text{A85})$$




$$\begin{aligned} \int_{-\infty}^{\infty} \frac{dp}{2\pi} \frac{\sin(pnL)}{[L\omega^{-2} + (p-q)^2][p^2 + \delta^2]} = \\ \frac{2e^{-nL\delta}L\omega^4 q - e^{-nL/L\omega}L\omega^3 \{2L\omega q \cos(qnL) + [1 - L\omega^2(q^2 + \delta^2)] \sin(qnL)\}}{2[1 + 2L\omega^2(q^2 - \delta^2) + L\omega^4(q^2 + \delta^2)^2]}. \end{aligned}$$

The last equation leads to:

$$\text{v.p.} \int_{-\infty}^{\infty} \frac{dk}{2\pi} \frac{\sin knL}{(k+q)^2(k^2 + L\omega^{-2})} = q \frac{1 - \exp[-nL/L\omega]}{(q^2 + L\omega^{-2})^2}, \quad q = 2\pi n/L, \quad n \in \mathbb{Z}, \quad \Re L\omega > 0. \quad (\text{A86})$$

References

- [1] Oleg Chalaev. Home page: <http://quantumtheory.physik.unibas.ch/shalaev/>.
- [2] Yoseph Imry. *Introduction to Mesoscopic Physics*. Oxford University Press, New York, 2002. .
- [3] M. Büttiker, Yoseph Imry, and Rolf Landauer. Josephson behavior in small normal one-dimensional rings. *Phys. Lett.*, 96A(7):365, July 1983.
- [4] Eberhard. K. Riedel and Felix von Oppen. Mesoscopic persistent current in small rings. *Phys. Rev. B*, 47(23):15449, Jun 1993.
- [5] Алексей Алексеевич Абрикосов, Лев Петрович Горьков, and Игорь Ехильевич Дзялошинский. *Methods of quantum field theory in statistical physics*. Dobrosvet (Moscow), 2nd Russian edition, 1998. Abrikosov, Gor'kov, Dzyaloshinskii, ; Numbering of formulas and, apparently, figures is the same, as in English edition.
- [6] Boris L. Altshuler and A. G. Aronov. Electron-electron interaction in disordered systems. In A. L. Efros and M. Pollak, editors, *Electron-electron interaction in disordered conductors*. Elsevier, 1985. .
- [7] Oleg Chalaev. Public version of unofficial notes.
- [8] Giuliano Benenti, Xavier Waintal, and Jean-Louis Pichard. A new quantum phase in two dimensions. *Rencontres de Moriond*, 1999. [cond-mat/9905028](#).
- [9] Ho-Fai Cheung, Eberhard K. Riedel, and Yuval Gefen. Persistent currents in mesoscopic rings and cylinders. *Phys. Rev. Lett.*, 62:587, Jan 1989.
- [10] Vinay Ambegaokar and Ulrich Eckern. Coherence and persistent currents in mesoscopic rings. *Phys. Rev. Lett.*, 65:381, 1990.
- [11] V. E. Kravtsov and V. I. Yudson. Direct current in mesoscopic rings induced by high-frequency electromagnetic field. *Phys. Rev. Lett.*, 70(2):210, Jan 1993.
- [12] Oleg L. Chalaev and V. E. Kravtsov. Persistent current in mesoscopic rings. was in preparation until I was at SISSA. The aim was to present the calculation of the triplet channel as well – see [31]; most probably, will never be published.
- [13] L. V. Keldysh. *ЖЭТФ*, 47:1515, 1964. *Zh. Eksp. Teor. Fiz.* **47**, 1515 (1964) [*Sov. Phys. JETP* **20**, 1018 (1965)].
- [14] Jørgen Rammer and H. Smith. Quantum field theoretical methods in transport theory of metals. *Rev. Mod. Phys.*, 58:323, 1986. .
- [15] Vladimir I. Yudson, Evgeni Kanzieper, and Vladimir E. Kravtsov. Limits of the dynamical approach to the nonlinear response of mesoscopic systems. *Phys. Rev. B*, 64:045310, 2001. [cond-mat/0012200](#); Статья, где ВК (и сотоварищи) объясняет, как можно считать проводимость по формуле Ландауэра в технике Келдыша.
- [16] Gabor Zala, Boris N. Narozhny, and Igor L. Aleiner. Interaction corrections at intermediate temperatures: I. longitudinal conductivity and kinetic equation. *Phys. Rev. B*, 64(21):214204, December 2001. [cond-mat/0105406](#); see also Proceedings of the International School of Physics in Varenna, Course CLI.
- [17] H. Pothier, S. Guéron, Norman O. Birge, D. Esteve, and M. H. Devoret. Energy distribution function of quasiparticles in mesoscopic wires. *Phys. Rev. Lett.*, 79(18):3490–3493, Nov 1997.
- [18] S. De Franceschi, R. Hanson, W. G. van der Wiel, J. M. Elzerman, J. J. Wijkema, T. Fujisawa, S. Tarucha, and L. P. Kouwenhoven. Kondo effect out of equilibrium in a mesoscopic device. [arXiv:cond-mat/0203146](#), Mar 2002.
- [19] Vladimir Yudson. unpublished; источник информации – ВК.
- [20] Л. Д. Ландау and Е. М. Лифшиц. *Статистическая физика. Часть 1.*, volume 5 of *Theoretical physics*. Наука, 1976.  Landau & Lifshitz V – “Statistical physics part 1”.
- [21] Фёдор Максимилианович Куни. *Статистическая физика и термодинамика*. Наука, 1981. .
- [22] В. Л. Бонч-Бруевич and С. В. Тябликов. *Метод функций Грина в статистической механике*. гос. изд. физ.-мат. лит., Москва, 1962. V. L. Bonch-Bruевич and S. V. Tyablikov, “The Green function method in statistical mechanics” .
- [23] Boris L. Altshuler, A. G. Aronov, and D. E. Khmelnitsky. Effects of electron-electron collisions with small energy transfers on quantum localization. *Journal of Physics C: Solid State Physics*, 15:7367–7386, 1982. .

- [24] A. D. Mirlin. unpublished.
- [25] Алексей Алексеевич Абрикосов. *Основы теории металлов*. Наука, 1987.  A. A. Abrikosov “Fundamentals of the Theory of Metals”.
- [26] Oleg Chalaev and Vladimir E. Kravtsov. Aharonov-Bohm magnetization of mesoscopic rings caused by inelastic relaxation. *Phys. Rev. Lett.*, 89:176601, 2002. [cond-mat/0204176](#).
- [27] Alexander L. Fetter and John Dirk Walecka. *Quantum theory of many-particle systems*. McGraw-Hill, San Francisco, 1971.
- [28] Boris L. Altshuler, Arkadi G. Aronov, and P. Lee. Interaction effects in disordered Fermi systems in 2 dimensions. *Phys. Rev. Lett.*, 44(19):1288–1291, 1980.  Correction to the conductivity taking into account interaction.
- [29] Л. Д. Ландау and Е. М. Лифшиц. *Квантовая механика (нерелятивистская теория)*, volume 3 of *Theoretical physics*. “Наука”, 4th Russian edition, 1989.  Landau & Lifshitz, “Quantum mechanics – non-relativistic theory”.
- [30] Barry R. Holstein. *Topics in advanced quantum mechanics*. Addison-Wesley, Redwood City, Calif., 1992.
- [31] Oleg Chalaev. *Nonequilibrium persistent currents in mesoscopic disordered systems*. PhD thesis, Scuola Internazionale Superiore di Studi Avanzati, Trieste, Italy, 2003. The thesis together with the presentation are available on my homepage [1].